Substitution of L-Trp by *α*-methyl-L-Trp in ^{177}Lu-RM2 results in ^{177}Lu-AMTG, a high affinity GRPR ligand with improved *in vivo* stability

Thomas Günther[1], Sandra Deiser[1], Veronika Felber[1], Roswitha Beck[1], and Hans-Jürgen Wester[1]

[1]Chair of Pharmaceutical Radiochemistry, Technical University of Munich, Garching, Germany

Corresponding author:

Thomas Günther, PhD

Phone: +49.89.289.12203

Fax: +49.89.289.12204

E-Mail: thomas.guenther@tum.de

ORCID: https://orcid.org/0000-0002-7412-0297

Address of corresponding author:

Technical University of Munich,

Chair of Pharmaceutical Radiochemistry,

Walther-Meissner-Str. 3

85748 Garching

GERMANY

Running title: *GRPR Ligands for Radioligand Therapy*

ABSTRACT

Theranostic applications targeting the gastrin-releasing peptide receptor (GRPR) have shown promising results. When compared with other peptide ligands for radioligand therapy, the most often used GRPR ligand, RM2 (DOTA-Pip^5-D-Phe^6-Gln^7-Trp^8-Ala^9-Val^{10}-Gly^{11}-His^{12}-Sta^{13}-Leu^{14}-NH$_2$), may be clinically impacted by limited metabolic stability. **Aim:** With the aim to improve the metabolic stability of RM2, we investigated whether the metabolically unstable Gln^7-Trp^8 bond within the pharmacophore of RM2 can be stabilized *via* substitution of L-Trp^8 by α-methyl-L-tryptophan (α-Me-L-Trp) and whether the corresponding DOTAGA analogue might also be advantageous. A comparative preclinical evaluation of ^{177}Lu-α-Me-L-Trp^8-RM2 (^{177}Lu-AMTG) and its DOTAGA counterpart (^{177}Lu-AMTG2) was carried out using ^{177}Lu-RM2 and ^{177}Lu-NeoBOMB1 as reference compounds. **Methods:** Peptides were synthesized by solid-phase peptide synthesis (SPPS) and labeled with ^{177}Lu. Lipophilicity was determined at pH 7.4 (log$D_{7.4}$). Receptor-mediated internalization was investigated on PC-3 cells (37 °C, 60 min), whereas GRPR affinity (IC_{50}) was determined on both PC-3 and T-47D cells. Stability towards peptidases was examined *in vitro* (human plasma, 37 °C, 72 ± 2 h) and *in vivo* (murine plasma, 30 min post injection (p.i.)). Biodistribution studies were carried out at 24 h p.i. and single photon emission tomography/computed tomography (μSPECT/CT) images in PC-3 tumor-bearing mice at 1, 4, 8, 24 and 28 h p.i. **Results:** Syntheses *via* SPPS yielded 9-15% purified labeling precursors. ^{177}Lu-labeling proceeded quantitatively. Compared to ^{177}Lu-RM2, ^{177}Lu-AMTG showed slightly improved GRPR affinity, a similar low internalization rate, slightly increased lipophilicity, and considerably improved stability *in vitro* and *in vivo*. *In vivo*, ^{177}Lu-AMTG exhibited the highest tumor retention (11.45 ± 0.43 %ID/g) and tumor/blood ratio (2702 ± 321) at 24 h p.i. as well as a favorable biodistribution profile. As demonstrated by μSPECT/CT imaging, ^{177}Lu-AMTG also revealed a less rapid clearance from tumor tissue. Compared to ^{177}Lu-AMTG, ^{177}Lu-AMTG2 did not show any further beneficial effects. **Conclusion:** The results of this study, particularly the superior metabolic stability of ^{177}Lu-AMTG, strongly recommend a clinical evaluation of this novel GRPR-targeted ligand to investigate its potential for radioligand therapy of GRPR-expressing malignancies.

INTRODUCTION

Radioligand therapy has emerged as a powerful alternative to conventional treatment options in oncology. This can mainly be attributed in case of neuroendocrine tumors to the success story of DOTATOC- and DOTATATE-based theranostics, and in the case of prostate cancer to prostate-specific membrane antigen (PSMA)-targeted inhibitors (*1,2*). Based on the overexpression of the gastrin-releasing peptide receptor (GRPR, Bombesin-2 receptor) in high density and high frequency already in early disease stages of prostate cancer (~5,000 dpm/mg [disintegrations per minute/milligram tissue]; >2000 dpm/mg considered as clinically relevant) and breast cancer (~10,000 dpm/mg), GRPR has been identified as a promising target for both cancer types(*3,4*).

In a recent study, 50 patients with biochemically recurrent prostate cancer were examined with either ^{68}Ga-PSMA11 or ^{18}F-DCFPyL positron emission tomography/computed tomography (PET/CT) and additionally with ^{68}Ga-RM2 PET/magnetic resonance imaging (PET/MRI). 36 lesions were only visible with ^{68}Ga-PSMA11/^{18}F-DCFPyL PET/CT, and seven only with ^{68}Ga-RM2 PET/MRI, which again suggests a complementary role of GRPR- and PSMA-targeted theranostics(*5*). Moreover, especially estrogen receptor-rich breast cancer (estrogen receptor expressed in over 80% of all breast cancers) shows high GRPR expression, which is retained in 95% of nodal metastases(*6,7*). Not surprisingly, successful high-contrasting PET imaging of breast cancer using ^{68}Ga-NOTA-RM26 or ^{68}Ga-RM2 has already been described(*8,9*).

The two most promising GRPR-targeted radiopharmaceuticals, ^{68}Ga-RM2 and ^{68}Ga-NeoBOMB1, already showed favorable initial results and are currently assessed in phase 1 and 2 clinical studies(*10-13*). A first in-man study on ^{177}Lu-RM2 in PSMA[-]/GRPR[+] prostate cancer patients revealed encouraging dosimetry data(*14*). Nevertheless, limited metabolic stability of some bombesin derivatives, such as RM2, is well-known and mainly caused by the neutral endopeptidase (NEP, EC 3.4.24.11), which reportedly cleaves linear peptides at the *N*-terminal side of hydrophobic amino acids(*15*). Incubation of ^{177}Lu-AMBA (DOTA-4-aminobenzoyl-Gln[7]-Trp[8]-Ala[9]-Val[10]-Gly[11]-His[12]-Leu[13]-Met[14]-NH$_2$) in murine and human plasma

in vitro revealed several cleavage sites, especially at the *C*-terminus and the Gln[7]-Trp[8] site(*16*). Similar observations were made in five healthy patients, as the administered ^{68}Ga-RM2 showed only 19% intact tracer in blood at 65 min p.i.(*17*). Considering this rather small fraction of intact compound early after injection, a metabolically stabilized RM2 analogue could result in improved tumor uptake, tumor retention and thus tumor dose. In recent years many groups developed bombesin analogues that were modified at the *C*- and/or *N*-termini, but not within the pharmacophoric sequence (Gln[7]-Trp[8]-Ala[9]-Val[10]-Gly[11]-His[12])(*18-22*).

As we hypothesize that the use of statine (i.e. Sta[13]) at the *C*-terminus of RM2 and its derivatives results in sufficient metabolic stabilization at this part of the molecule, we concluded that further improvements might be possible by stabilizing the Gln[7]-Trp[8] sequence. For this purpose, we substituted L-Trp[8] by α-methyl-L-tryptophan (α-Me-L-Trp) in ^{177}Lu-RM2 and its DOTAGA analogue (Fig. 1) and evaluated these novel compounds alongside the potent reference ligands ^{177}Lu-RM2 and ^{177}Lu-NeoBOMB1. The comparative preclinical evaluation comprises affinity studies (*IC*$_{50}$) on PC-3 and T-47D cells, quantification of receptor-mediated internalization on PC-3 cells, determination of log$D_{7.4}$, investigations on the stability against peptidases *in vitro* in human plasma and *in vivo* in plasma and urine of mice as well as biodistribution studies in PC-3 tumor-bearing mice.

MATERIALS AND METHODS

Chemical Synthesis and Labeling Procedures

RM2 derivatives were prepared *via* standard Fmoc-based SPPS using a *H*-Rink amide ChemMatrix® resin (35-100 mesh particle size, 0.4-0.6 mmol/g loading, *Merck KGaA*, Darmstadt, Germany). NeoBOMB1 was synthesized according to a reported procedure(*20*). Purification was accomplished by reversed phase high performance liquid chromatography (RP-HPLC).

Both [nat]Lu- and ^{177}Lu-labeling was prepared according to a modified procedure(*23*). The radiolabeled reference 3-^{125}I-D-Tyr[6]-MJ9 (Supplemental Figs. 1 and 2) was prepared according to a reported procedure(*24*). Detailed description of the synthesis, labeling and

characterization of RM2 and its analogues is provided in the Supplementary Information (Supplemental Figs. 3-12).

In Vitro Experiments

Detailed description of all cell-based experiments is provided in the Supplementary Information.

Affinity Determinations (IC$_{50}$) and Internalization Studies. Competitive binding studies were performed on both PC-3 and T-47D cells (1.5×10^5 cells in 1 mL/well) *via* incubation at room temperature for 2 h using 3-^{125}I-D-Tyr^6-MJ9 (0.2 nM/well) as radiolabeled reference (n = 3). Internalization studies of the ^{177}Lu-labeled conjugates (1.0 nM/well) were performed on PC-3 cells (1.5×10^5 cells in 1 mL/well) at 37 °C for 1 h (n = 6). Data were corrected for non-specific binding (competition by 10^{-3} M ^{nat}Lu-RM2).

Determination of Lipophilicity (n-octanol-PBS distribution coefficient, logD$_{7.4}$). Approximately 1 MBq of the ^{177}Lu-labeled compound was dissolved in 1 mL of phosphate buffered saline (PBS, pH = 7.4) and *n*-octanol (*v*/*v* = 1/1). After vortexing for 3 min at room temperature and subsequent centrifugation at 9000 rpm for 5 min (Biofuge 15, *Heraeus Sepatech GmbH*, Osterode, Germany), 200 µL aliquots of both layers were measured separately in a *γ*-counter. The experiment was repeated at least five times.

In Vitro Stability Studies. Metabolic stability *in vitro* was determined applying a procedure published by *Linder et al.* that was slightly modified(*16*). Immediately after labeling, 200 µL of human plasma were added and the mixture was incubated at 37 °C for 72 ± 2 h. Proteins were precipitated by treatment with ice-cold EtOH (150 µL) and ice-cold MeCN (450 µL), followed by centrifugation (13000 rpm, 20 min). The supernatants were decanted and further centrifuged (13000 rpm, 10 min) using a Costar® Spin-X® centrifuge tube filter (0.45 µm). The filtrated plasma samples were analyzed using radio RP-HPLC.

In Vivo Experiments

All animal experiments were conducted in accordance with general animal welfare regulations in Germany (German animal protection act, as amended on 18.05.2018, Art. 141

G v. 29.3.2017 I 626, approval no. ROB-55.2-2532.Vet_02-18-109) and the institutional guidelines for the care and use of animals.

In Vivo Stability Studies. Approximately 30-40 MBq (1 nmol, 150 µL) of the ^{177}Lu-labeled compounds were injected into the tail vein of anaesthetized CB17-SCID mice (n = 3). Following euthanasia at 30 min p.i., blood and urine samples were collected. Blood proteins were precipitated by treatment with ice-cold MeCN (*v*/*v* = 1/1), followed by centrifugation (13000 rpm, 20 min). The supernatants were decanted and further centrifuged (13000 rpm, 10 min) using a Costar® Spin-X® centrifuge tube filter (0.45 µm). The filtrated plasma samples as well as the urine samples were analyzed using radio RP-HPLC.

Biodistribution and µSPECT/CT Imaging Studies. Detailed description of tumor inoculation is provided in the Supplementary Information. Approximately 2–5 MBq (100 pmol, 150 µL) of the ^{177}Lu-labeled GRPR ligands were injected into the tail vein of anaesthetized (2% isoflurane) PC-3 tumor-bearing mice (biodistribution: n = 4, imaging: n = 1).

For biodistribution studies, organs were removed, weighted and measured in a *γ*-counter (*Perkin Elmer*, Waltham, MA, USA) following euthanasia at 24 h p.i.

Imaging studies were performed on a MILabs VECTor^4 small-animal SPECT/PET/optical imaging (OI)/CT device (*MILabs*, Utrecht, the Netherlands). Data were reconstructed using the MILabs Rec software (version 10.02) and a pixel-based Similarity-Regulated Ordered Subsets Expectation Maximization (SROSEM) algorithm, followed by data analysis using the PMOD4.0 software (*PMOD TECHNOLOGIES LLC*, Zurich, Switzerland). Static images were recorded at t = 1, 4, 8, 24 and 28 h p.i. with an acquisition time of t + (45-60 min) using the HE-GP-RM collimator and a step-wise multi-planar bed movement.

For all competition studies, 3.62 mg/kg (40 nmol) of ^{nat}Lu-RM2 (10^{-3} M in PBS) were co-administered.

RESULTS

Synthesis and Radiolabeling

Synthesis of uncomplexed ligands was carried out *via* standard Fmoc-based SPPS, yielding 9-15% of each labeling precursor after purification by RP-HPLC (chemical purity >98%, determined by RP-HPLC at $\lambda = 220$ nm). Complexation of all ligands with a 2.5-fold excess of $^{nat}LuCl_3$ resulted in quantitative yields. The remaining free Lu^{3+} did not affect the cell-based assay in a brief competition study (Supplemental Fig. 13), thus purification prior to affinity studies was dispensed. ^{125}I-Iodination of D-Tyr^6-MJ9 by means of the Iodo-Gen$^®$ method resulted in 3-^{125}I-D-Tyr^6-MJ9 with radiochemical yields (RCY) of 33-48% and radiochemical purities (RCP) of >98% after RP-HPLC purification. ^{177}Lu-labeling of all compounds was performed manually, each resulting in quantitative RCYs, RCPs of >98% and molar activities of 40 ± 10 GBq/µmol. All ^{177}Lu-labeled ligands were used without further purification.

In Vitro Characterization

In vitro data of the examined bombesin-based ligands are summarized in Figure 2 and Supplemental Table 1. The cold counterpart of 3-^{125}I-D-Tyr^6-MJ9 showed an IC_{50} of 1.3 ± 0.4 nM on PC-3 cells. The ^{nat}Lu-labeled compounds exhibited IC_{50} values in a range of 3.0-4.7 on PC-3 and 1.0-4.6 nM on T-47D cells. ^{177}Lu-α-Me-L-Trp^8-RM2 ($=^{177}Lu$-AMTG) and ^{177}Lu-RM2 were internalized by PC-3 cells within 1 h in similar amounts (3.03 ± 0.18 vs. $2.92 \pm 0.20\%$). ^{177}Lu-DOTAGA-α-Me-L-Trp^8-RM2 ($=^{177}Lu$-AMTG2) ($5.88 \pm 0.33\%$) and ^{177}Lu-NeoBOMB1 ($13.91 \pm 0.64\%$) were taken up in higher amounts. Whereas the distribution coefficients ($\log D_{7.4}$) were quite similar for ^{177}Lu-RM2 and its analogues (−2.3 to −2.5), ^{177}Lu-NeoBOMB1 was found to be considerably more lipophilic (−0.57 ± 0.03). Highest amounts of intact compound *in vitro* in human plasma was found for ^{177}Lu-AMTG ($77.7 \pm 8.7\%$). Whereas ^{177}Lu-AMTG2 and ^{177}Lu-NeoBOMB1 exhibited only a slightly reduced stability *in vitro* (66.2 ± 5.1 vs. $61.9 \pm 2.1\%$), only $38.7 \pm 9.3\%$ intact ^{177}Lu-RM2 was found after incubation in human plasma for 72 ± 2 h (Fig. 2; Supplemental Fig. 14).

In Vivo Characterization

In vivo stability in murine plasma at 30 min p.i. was highest for ^{177}Lu-AMTG (92.9 ± 0.7% intact tracer). Again, slightly decreased metabolic stability was observed for ^{177}Lu-NeoBOMB1 (75.9 ± 0.6%) and ^{177}Lu-AMTG2 (77.6 ± 3.1%), whereas ^{177}Lu-RM2 was found to be quite unstable (11.4 ± 3.7%). In addition to these findings, ^{177}Lu-AMTG and ^{177}Lu-AMTG2 were found to be excreted into the urine at 30 min p.i. predominantly as intact tracers (68.2 ± 3.1 and 61.6 ± 1.6%, respectively) (Fig. 2; Supplemental Figs. 15 and 16). Interestingly, after injection of ^{177}Lu-RM2 and ^{177}Lu-NeoBOMB1 radioactivity appears in the urine almost quantitatively in the form of their metabolites (0.5 ± 0.1 vs. 3.9 ± 1.3% intact tracer).

Biodistribution studies in PC-3 tumor-bearing mice were carried out at 24 h p.i. (Table 1). ^{177}Lu-RM2 and its derivatives revealed low activity levels in most organs at 24 h p.i., indicating a rapid clearance from non-tumor tissue, which is especially important for blood and GRPR$^+$ organs such as pancreas and intestine. ^{177}Lu-NeoBOMB1 showed increased activity levels in several non-tumor organs at 24 h p.i., particularly in lung, liver, spleen, pancreas, intestine and adrenals. Bone uptake was slightly enhanced for ^{177}Lu-RM2, which was attributed to incomplete labeling (RCY~95%, chromatogram not shown) and thus free [177]LuCl$_3$. Tumor retention was comparable for all compounds except for ^{177}Lu-AMTG, which exhibited distinctly increased values at 24 h p.i. (7.2-8.5 vs. 11.5 percent injected dose per gram; %ID/g). Not surprisingly, ^{177}Lu-AMTG showed the highest tumor/background ratios at 24 h p.i. The tumor/blood ratio of ^{177}Lu-AMTG (2702 ± 321) was almost four times higher than that of ^{177}Lu-RM2 and ^{177}Lu-AMTG2, and approximately 15-times higher than that of ^{177}Lu-NeoBOMB1 (Supplemental Table 2).

*μ*SPECT/CT studies with ^{177}Lu-RM2 and ^{177}Lu-AMTG at 1, 4, 8, 24 and 28 h p.i. in PC-3 tumor-bearing mice revealed low background activity levels for both tracers at time points ≥4 h and considerably higher activity accumulation in both tumor and pancreas for ^{177}Lu-AMTG (Fig. 3). For both tracers, specificity of tumor uptake was confirmed *via* competition experiments with excess of [nat]Lu-RM2 (Table 1; Supplemental Fig. 17).

DISCUSSION

With regard to radioligand therapy, the two most promising GRPR ligands, ^{68}Ga-RM2 and ^{68}Ga-NeoBOMB1, present some disadvantages: ^{68}Ga-RM2 suffers from rapid metabolic degradation[17], which is why tumor accumulation and tumor dose for ^{177}Lu-RM2 is likely limited as well, especially important in the context of radioligand therapy. In contrast, ^{177}Lu-NeoBOMB1, which exhibits a higher metabolic stability *in vivo*, shows enhanced activity retention in tumor tissue, but also in blood[19]. This results in unfavorable dosimetry and higher doses to the red bone marrow[25]. With the aim of retaining the excellent pharmacokinetics of RM2, we substituted the metabolically less stable Gln^7-Trp^8 sequence of ^{177}Lu-RM2 and its DOTAGA analogue by the unnatural amino acid *α*-methyl-L-tryptophan, and compared these new ligands with ^{177}Lu-RM2 and ^{177}Lu-NeoBOMB1 as references.

Synthesis was easily accessible *via* SPPS and complexation with [nat]Lu or ^{177}Lu proceeded quantitatively. All four compounds contain a similar pharmacophore typical for bombesin analogues, resulting in high affinities that were in the range of IC_{50} values reported for [nat]In-RM2 (9.3 nM), several [nat]Ga-RM26 derivatives (2.3-10.0 nM), [nat]Ga-NeoBOMB1 (2.5 nM) or SB3 (3.5 nM)[18,19,21,26]. Apart from [nat]Lu-AMTG2, higher cellular uptake of 3-^{125}I-D-Tyr^6-MJ9 as well as slightly elevated IC_{50} values on PC-3 compared to on T-47D cells was observed (Supplemental Figs. 18 and 19), which was attributed to an increased number of receptors present on PC-3 cells.

We could show that *α*-methyl-L-Trp-for-L-Trp^8 and DOTAGA-for-DOTA substitution had only minimal impact on GRPR affinity, lipophilicity ($logD_{7.4}$) and receptor-mediated internalization, demonstrating that these modifications might allow to keep the *in vivo* kinetics of ^{177}Lu-RM2 almost unaffected. In contrast, higher internalization levels and lipophilicity already indicate the *in vivo* limitations of ^{177}Lu-NeoBOMB1.

Besides retaining the favorable *in vitro* data of ^{177}Lu-RM2, the primary aim of this study was to chemically stabilize the Gln-Trp bond to potentially improve its longtime behavior *in vivo*. Comparative stability studies *in vitro* and *in vivo* as well as the resulting biodistribution profiles substantiated our working hypothesis of addressing the major metabolic instability at

the Gln-Trp site in RM2 and other bombesin-like compounds. Both ^{177}Lu-AMTG and ^{177}Lu-AMTG2 exhibited equal or even higher amounts of intact compound in human plasma *in vitro* and in murine plasma and urine *in vivo* than the two references. For ^{68}Ga-RM2 and ^{177}Lu-NeoBOMB1, the fraction of intact tracer in murine blood was reported to be 55% (15 min p.i.)(*27*) and 90% (30 min p.i.)(*19*), respectively, which is lower than the value we determined for ^{177}Lu-AMTG (30 min p.i.).

Unlike *Linder et al.* in a stability study on ^{177}Lu-AMBA(*16*), we observed less metabolites for each ligand after incubation in human plasma (Supplemental Fig. 14), which can be explained by the *C*-terminal modifications present in each of the four compounds tested in this study. *Popp et al.* observed one major and two minor metabolites for ^{68}Ga-RM2 in murine plasma at 15 min p.i.(*27*), while we detected only one major and one minor metabolite for ^{177}Lu-RM2 at 30 min p.i. This could be either due to our analysis method or the effect reported by *Linder et al.* that the minor metabolites can be further metabolized to yield the major metabolite, the longer the circulation *in vivo* takes place.

Not surprisingly, increased metabolic stability observed in human and murine plasma for ^{177}Lu-AMTG resulted in a 35% higher activity level in tumor compared to ^{177}Lu-RM2 in PC-3 tumor-bearing mice at 24 h p.i. (Fig. 4). Both ^{177}Lu-AMTG and ^{177}Lu-AMTG2 exhibited excellent clearance kinetics and thus low activity levels in non-tumor organs, with the highest values obtained for the kidneys (1.2-1.9 %ID/g). Both compounds were mostly cleared intact (Supplemental Fig. 16), which could be favorable over ^{177}Lu-RM2 and ^{177}Lu-NeoBOMB1, as charged metabolites tend to be taken up and retained in the kidneys. Most importantly, activity concentration in blood as well as for the GRPR[+] pancreas was low for all ^{177}Lu-RM2 analogs at 24 h p.i. (<0.01 and <1 %ID/g, respectively), which we considered as another prerequisite for a successful translation into men.

In contrast, ^{177}Lu-NeoBOMB1 displayed enhanced activity levels in most non-tumor organs and thus the lowest tumor/background ratios in most organs, especially in blood, liver, spleen, pancreas and adrenals, which was also observed by other groups(*19,25*). The biodistribution profiles confirmed our concerns regarding its increased lipophilicity and

internalization rates. It might be speculated that retention in the GRPR[+] pancreas could be caused by a partial agonistic behavior observed in our internalization study, since GRPR agonists such as PESIN or AMBA that exhibit internalization rates >25% at 1 h *in vitro* typically show a slow clearance from the pancreas over time(*28,29*).

Although a reduced internalization might be caused by other reasons, the high structural similarity of ^{177}Lu-AMTG/^{177}Lu-AMTG2 to the known GRPR antagonist ^{177}Lu-RM2 and the comparably low internalization pattern observed in our studies is a strong indicator towards antagonistic behavior of these new compounds. This assumption is further corroborated by rapid pancreatic clearance within 24 h p.i. and the thus resulting favorable biodistribution profiles. This was also evident in *μ*SPECT/CT scans with ^{177}Lu-RM2 and ^{177}Lu-AMTG over time, in which both demonstrated high tumor retention and fast clearance from non-tumor organs, even the GRPR[+] pancreas. Noteworthy, clearance from pancreas and tumor was less rapid for ^{177}Lu-AMTG, which confirmed our hypothesis on increased metabolic stability *in vivo* generated by a simple modification at the Trp[8] site. Thus not surprising, tumor/background ratios for ^{177}Lu-AMTG were highest in all organs, except for the tumor/muscle ratio (Fig. 5).

Regarding dose limiting organs in the context of radioligand therapy, the excellent tumor/kidney and tumor/blood ratios make ^{177}Lu-AMTG a highly attractive alternative to ^{177}Lu-RM2 (*30*). In fact, ^{177}Lu-AMTG seems to synergistically combine the advantages of ^{177}Lu-RM2 and ^{177}Lu-NeoBOMB1 regarding pharmacokinetics and stability, while simultaneous offering the best GRPR affinity, both on PC-3 and T-47D cells. Thus, a clinical assessment (e.g. clinical phase I study) with ^{177}Lu-AMTG seems to be warranted.

In summary, we were able to successfully introduce an *α*-methyl-L-Trp-for-L-Trp[8] substitution within the pharmacophore of ^{177}Lu-RM2 that not only resulted in a new tracer (^{177}Lu-AMTG) with comparable affinity, internalization and lipophilicity, but also in considerably improved metabolic stability. Hence, improved tumor uptake and pharmacokinetics superior to that of the parent peptide ^{177}Lu-RM2 or the second reference compound, ^{177}Lu-NeoBOMB1, were observed for ^{177}Lu-AMTG. Noteworthy, improved metabolic stability was achieved without

12

co-administration of peptidase inhibitors(*21*), such as phosphoramidon, which could facilitate a clinical translation. It seems legitimate to conclude that other bombesin derivatives published in recent years, which have been modified at the *N-* or *C-*terminus but not at the unstable dipeptide sequence Gln[7]-Trp[8](*20-22*), would also benefit from an *α*-methyl-L-Trp-for-L-Trp[8] substitution. Nevertheless, studies in prostate and breast cancer patients have to be carried out to show whether these promising preclinical results are reflected on a clinical level.

CONCLUSION

We could demonstrate that the new ^{177}Lu-RM2 derivative ^{177}Lu-AMTG offers a better overall preclinical performance than ^{177}Lu-RM2 and ^{177}Lu-NeoBOMB1. Based on these results, a clinical translation of ^{177}Lu-AMTG is highly recommended to assess a potential improved therapeutic value for radioligand therapy of GRPR-expressing malignancies, such as prostate and breast cancer.

In addition, we expect that the substitution of L-amino acids by their corresponding *α*-alkyl-L-amino acid analogues could also be a valuable approach to stabilize the pharmacophore of other peptidic ligands that suffer from insufficient stability *in vivo.*

DISCLOSURE

ACKNOWLEDGMENTS

KEY POINTS

QUESTION: Is it possible to overcome the major limitation of ^{177}Lu-RM2, its metabolic instability, with regard to future GRPR-targeted radioligand therapy by means of a tiny modification without negatively influencing overall pharmacokinetics?

PERTINENT FINDINGS: Substitution of L-Trp^8 by α-methyl-L-Trp^8 in the pharmacophoric sequence of ^{177}Lu-RM2 retains the favorable tracer pharmacokinetics while leading to an enhanced metabolic stability, making ^{177}Lu-AMTG a highly promising novel GRPR-targeted radiopharmaceutical for radioligand therapy.

IMPLICATIONS FOR PATIENT CARE: Although the clinical value of ^{177}Lu-AMTG has to be determined in clinical studies, this study could open new possibilities for complementary treatment of prostate and breast cancer.
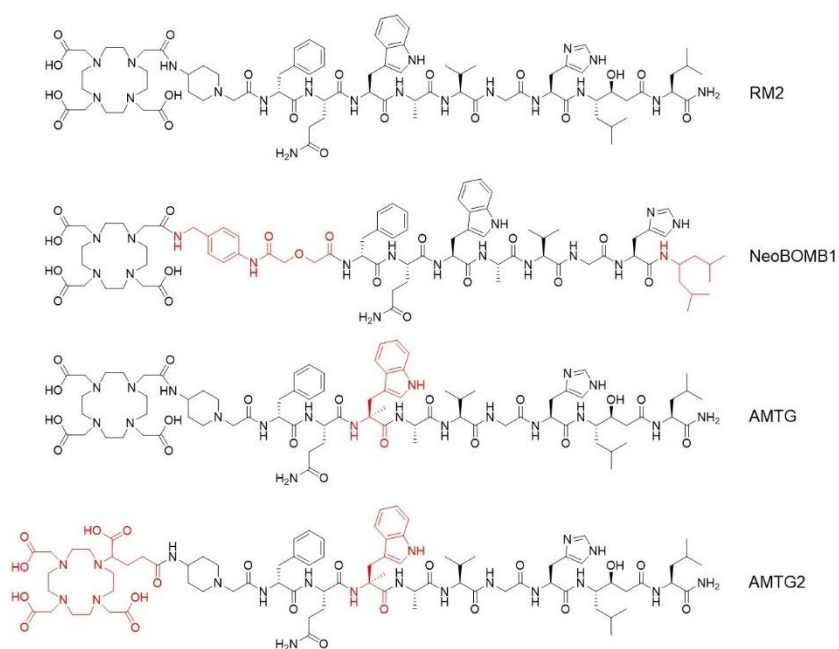
REFERENCES

1. Maqsood MH, Tameez Ud Din A, Khan AH. Neuroendocrine tumor therapy with lutetium-177: a literature review. *Cureus.* 2019;11:e3986.

2. Rahbar K, Afshar-Oromieh A, Jadvar H, Ahmadzadehfar H. PSMA theranostics: current status and future directions. *Mol Imaging.* 2018;17:1536012118776068.

3. Reubi JC, Wenger S, Schmuckli-Maurer J, Schaer JC, Gugger M. Bombesin receptor subtypes in human cancers: detection with the universal radioligand (125)I-[D-TYR(6), beta-ALA(11), PHE(13), NLE(14)] bombesin(6-14). *Clin Cancer Res.* 2002;8:1139-1146.

4. Reubi C, Gugger M, Waser B. Co-expressed peptide receptors in breast cancer as a molecular basis for in vivo multireceptor tumour targeting. *Eur J Nucl Med Mol Imaging.* 2002;29:855-862.

5. Baratto L, Song H, Duan H, et al. PSMA- and GRPR-targeted PET: results from 50 patients with biochemically recurrent prostate cancer. *J Nucl Med.* 2021;62:1545-1549.

6. Dalm SU, Sieuwerts AM, Look MP, et al. Clinical relevance of targeting the gastrin-releasing peptide receptor, somatostatin receptor 2, or chemokine C-X-C motif receptor 4 in breast cancer for imaging and therapy. *J Nucl Med.* 2015;56:1487-1493.

7. Morgat C, MacGrogan G, Brouste V, et al. Expression of gastrin-releasing peptide receptor in breast cancer and its association with pathologic, biologic, and clinical parameters: a study of 1,432 primary tumors. *J Nucl Med.* 2017;58:1401-1407.

8. Zang J, Mao F, Wang H, et al. 68Ga-NOTA-RM26 PET/CT in the evaluation of breast cancer: a pilot prospective study. *Clin Nucl Med.* 2018;43:663-669.

9. Stoykow C, Erbes T, Maecke HR, et al. Gastrin-releasing peptide receptor imaging in breast cancer using the receptor antagonist (68)Ga-RM2 and PET. *Theranostics.* 2016;6:1641-1650.

10. 68-Ga-RM2 PET/MRI in imaging patients with estrogen receptor-positive breast cancer. https://ClinicalTrials.gov/show/NCT03831711. Accessed February 26, 2020.

11. 68Ga-RM2 PET/CT in detecting regional nodal and distant metastases in patients with intermediate or high-risk prostate cancer. https://ClinicalTrials.gov/show/NCT03113617. Accessed February 26, 2020.

12. 68Ga-RM2 PET/MRI in biochemically recurrent prostate cancer. https://ClinicalTrials.gov/show/NCT02624518. Accessed February 26, 2020.

13. 177Lu-NeoB in patients with advanced solid tumors and with 68Ga-NeoB lesion uptake. https://ClinicalTrials.gov/show/NCT03872778. Accessed February 26, 2020.

14. Kurth J, Krause BJ, Schwarzenböck SM, Bergner C, Hakenberg OW, Heuschkel M. First-in-human dosimetry of gastrin-releasing peptide receptor antagonist [(177)Lu]Lu-RM2: a radiopharmaceutical for the treatment of metastatic castration-resistant prostate cancer. *Eur J Nucl Med Mol Imaging.* 2020;47:123-135.

15. Shipp MA, Tarr GE, Chen CY, et al. CD10/neutral endopeptidase 24.11 hydrolyzes bombesin-like peptides and regulates the growth of small cell carcinomas of the lung. *Proc Natl Acad Sci U S A.* 1991;88:10662-10666.

16. Linder KE, Metcalfe E, Arunachalam T, et al. In vitro and in vivo metabolism of Lu-AMBA, a GRP-receptor binding compound, and the synthesis and characterization of its metabolites. *Bioconjug Chem.* 2009;20:1171-1178.

17. Roivainen A, Kahkonen E, Luoto P, et al. Plasma pharmacokinetics, whole-body distribution, metabolism, and radiation dosimetry of 68Ga bombesin antagonist BAY 86-7548 in healthy men. *J Nucl Med.* 2013;54:867-872.

18. Mansi R, Wang X, Forrer F, et al. Development of a potent DOTA-conjugated bombesin antagonist for targeting GRPr-positive tumours. *Eur J Nucl Med Mol Imaging.* 2011;38:97-107.

19. Kaloudi A, Lymperis E, Giarika A, et al. NeoBOMB1, a GRPR-antagonist for breast cancer theragnostics: first results of a preclinical study with [(67)Ga]NeoBOMB1 in T-47D cells and tumor-bearing mice. *Molecules.* 2017;22.

20. Lau J, Rousseau E, Zhang Z, et al. Positron emission tomography imaging of the gastrin-releasing peptide receptor with a novel bombesin analogue. *ACS Omega.* 2019;4:1470-1478.

21. Bakker IL, van Tiel ST, Haeck J, et al. In vivo stabilized SB3, an attractive GRPR antagonist, for pre- and intra-operative imaging for prostate cancer. *Mol Imaging Biol.* 2018;20:973-983.

22. Mitran B, Thisgaard H, Rosenstrom U, et al. High contrast PET imaging of GRPR expression in prostate cancer using cobalt-labeled bombesin antagonist RM26. *Contrast Media Mol Imaging.* 2017;2017:6873684.

23. Weineisen M, Simecek J, Schottelius M, Schwaiger M, Wester HJ. Synthesis and preclinical evaluation of DOTAGA-conjugated PSMA ligands for functional imaging and endoradiotherapy of prostate cancer. *EJNMMI Res.* 2014;4:63.

24. Nakagawa T, Hocart SJ, Schumann M, et al. Identification of key amino acids in the gastrin-releasing peptide receptor (GRPR) responsible for high affinity binding of gastrin-releasing peptide (GRP). *Biochem Pharmacol.* 2005;69:579-593.

25. Dalm SU, Bakker IL, de Blois E, et al. 68Ga/177Lu-NeoBOMB1, a novel radiolabeled GRPR antagonist for theranostic use in oncology. *J Nucl Med.* 2017;58:293-299.

26. Varasteh Z, Mitran B, Rosenstrom U, et al. The effect of macrocyclic chelators on the targeting properties of the 68Ga-labeled gastrin releasing peptide receptor antagonist PEG2-RM26. *Nucl Med Biol.* 2015;42:446-454.

27. Popp I, Del Pozzo L, Waser B, et al. Approaches to improve metabolic stability of a statine-based GRP receptor antagonist. *Nucl Med Biol.* 2017;45:22-29.

28. Mansi R, Wang X, Forrer F, et al. Evaluation of a 1,4,7,10-tetraazacyclododecane-1,4,7,10-tetraacetic acid-conjugated bombesin-based radioantagonist for the labeling with single-photon emission computed tomography, positron emission tomography, and therapeutic radionuclides. *Clin Cancer Res.* 2009;15:5240-5249.

29. Zhang H, Schuhmacher J, Waser B, et al. DOTA-PESIN, a DOTA-conjugated bombesin derivative designed for the imaging and targeted radionuclide treatment of bombesin receptor-positive tumours. *Eur J Nucl Med Mol Imaging.* 2007;34:1198-1208.

30. Coleman CN, Blakely WF, Fike JR, et al. Molecular and cellular biology of moderate-dose (1-10 Gy) radiation and potential mechanisms of radiation protection: report of a workshop at Bethesda, Maryland, December 17-18, 2001. *Radiat Res.* 2003;159:812-834.

FIGURE 1. Chemical structure of RM2 and its *α*-methyl-L-tryptophan (*α*-Me-L-Trp[8]) modified derivatives AMTG and AMTG2 as well as the reference ligand NeoBOMB1. Structural differences to RM2 are highlighted in red.
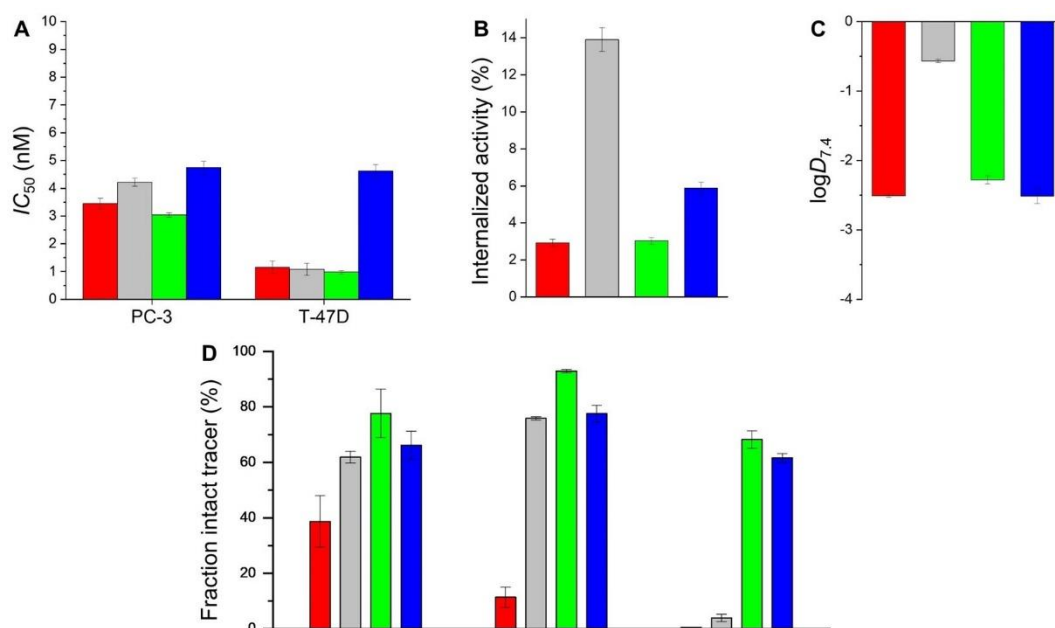
FIGURE 2. Preclinical data of $^{nat/177}$Lu-RM2 (red), $^{nat/177}$Lu-NeoBOMB1 (grey), $^{nat/177}$Lu-AMTG (green) and $^{nat/177}$Lu-AMTG2 (blue). (A) Affinity data on PC-3 and T-47D cells (1.5×10^5 cells/mL/well) using 3-^{125}I-D-Tyr^6-MJ9 (c = 0.2 nM) as radiolabeled reference (2 h, rt, HBSS + 1% BSA, v/v). (B) GRPR-mediated internalization (0.25 pmol/well) on PC-3 cells as percent (%) of applied activity (incubation at 37 °C for 1 h, DMEM/F-12 + 5% BSA (v/v), 1.5×10^5 cells/mL/well). Data corrected for non-specific binding (10^{-3} M ^{nat}Lu-RM2). (C) Lipophilicity at pH 7.4 ($\log D_{7.4}$). (D) Metabolic stability *in vitro* in human plasma (left) (37 °C, 72 ± 2 h; n = 4). Metabolic stability *in vivo* in murine plasma (middle) and murine urine (right) at 30 min p.i. (n = 3). Data expressed as mean ± SD. Metabolic stability of the ^{177}Lu-RM2 derivatives as determined *in vitro* and *in vivo*.
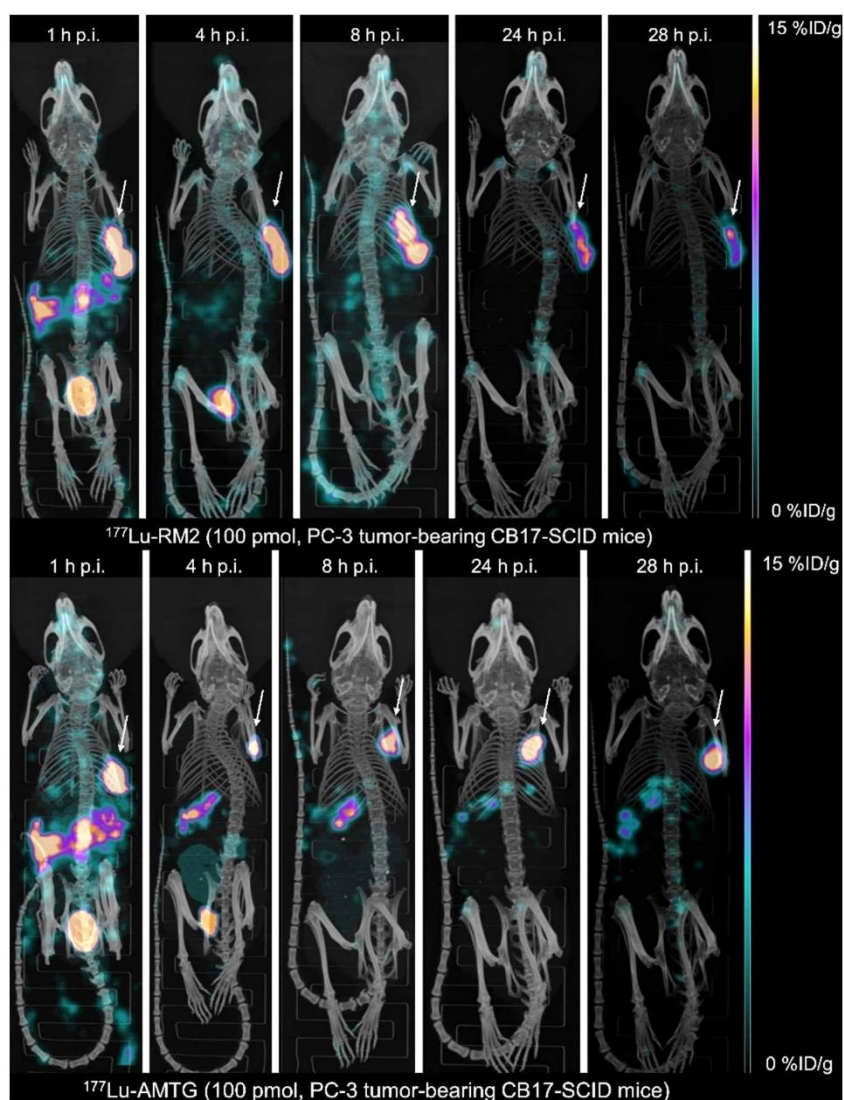
FIGURE 3. Maximum intensity projection of PC-3 tumor-bearing CB17-SCID mice injected with ^{177}Lu-RM2 (top) and ^{177}Lu-AMTG (bottom) (100 pmol each). Images were acquired at 1, 4, 8, 24 and 28 h p.i. into PC-3 tumors (white arrows).
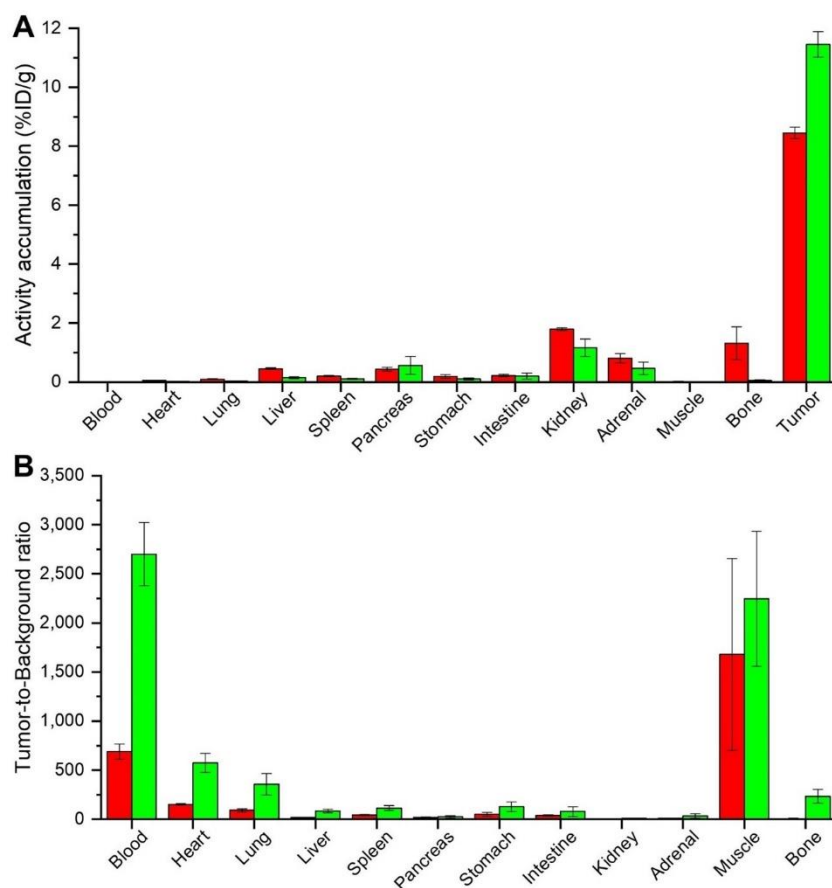
FIGURE 4. (A) Biodistribution of ^{177}Lu-RM2 (red) and ^{177}Lu-AMTG (green) in selected organs at 24 h p.i. in PC-3 tumor-bearing CB17-SCID mice (100 pmol each). Data expressed in %ID/g, mean ± SD (n = 4). (B) Tumor/background ratios for the selected organs for ^{177}Lu-RM2 (red) and ^{177}Lu-AMTG (green) at 24 h p.i. in PC-3 tumor-bearing CB17-SCID mice. Data are expressed as mean ± SD (n = 4).
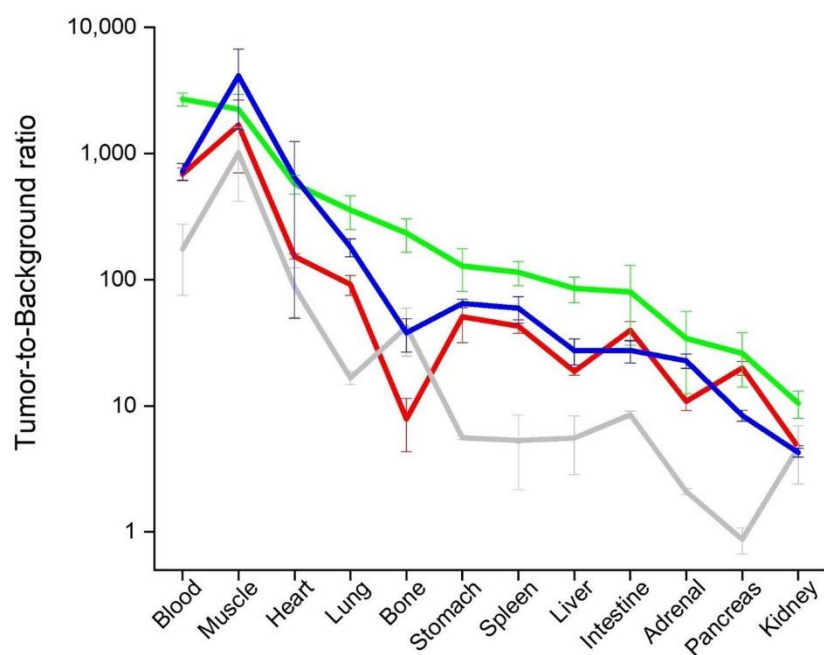
FIGURE 5. Graphical comparison of tumor/background ratios for the selected organs for ^{177}Lu-RM2 (red), ^{177}Lu-NeoBOMB1 (grey), ^{177}Lu-AMTG (green) and ^{177}Lu-AMTG (blue). Biodistribution studies were carried out at 24 h p.i. in PC-3 tumor-bearing CB17-SCID mice. Data are expressed as mean ± SD (n = 4).

TABLES

TABLE 1. Biodistribution of ^{177}Lu-RM2, ^{177}Lu-NeoBOMB1, ^{177}Lu-AMTG and ^{177}Lu-AMTG2 in selected organs at 24 h p.i. in PC-3 tumor-bearing CB17-SCID mice (100 pmol each). Data are expressed as %ID/g, mean ± SD (n = 4). Competition studies were carried out by co-injection of [nat]Lu-RM2 (3.62 mg/kg; mean ± SD, n = 3).

Organ	^{177}Lu-RM2	^{177}Lu-NeoBOMB1	^{177}Lu-AMTG	^{177}Lu-AMTG -competition study-	^{177}Lu-AMTG2	^{177}Lu-AMTG2 -competition study-
Blood	0.012±0.001	0.057±0.027	0.004±0.001	0.003±0.000	0.011±0.000	0.002±0.001
Heart	0.06±0.00	0.10±0.03	0.02±0.00	0.02±0.01	0.03±0.02	0.02±0.01
Lung	0.10±0.02	0.43±0.00	0.04±0.01	0.27±0.15	0.05±0.01	1.18±1.49
Liver	0.45±0.03	1.60±0.62	0.14±0.03	1.40±0.86	0.32±0.14	0.74±0.44
Spleen	0.20±0.02	1.94±0.97	0.10±0.02	2.97±2.01	0.15±0.07	1.06±1.08
Pancreas	0.43±0.06	8.48±0.92	0.56±0.30	0.05±0.03	0.95±0.14	0.07±0.01
Stomach	0.19±0.06	1.29±0.12	0.10±0.04	0.04±0.02	0.12±0.03	0.04±0.01
Intestine	0.22±0.04	0.85±0.05	0.20±0.10	0.27±0.21	0.30±0.04	0.34±0.35
Kidney	1.79±0.05	1.90±0.72	1.16±0.20	1.17±0.26	1.87±0.27	1.63±0.44
Adrenal	0.80±0.16	3.44±0.25	0.46±0.22	0.09±0.07	0.26±0.14	0.03±0.02
Muscle	0.011±0.011	0.010±0.005	0.005±0.003	0.003±0.002	0.003±0.003	0.003±0.002
Bone	1.31±0.56	0.20±0.06	0.05±0.02	0.05±0.03	0.22±0.05	0.02±0.01
Tumor	8.45±0.19	7.23±0.91	11.45±0.43	0.33±0.20	7.97±1.34	0.36±0.25

GRAPHICAL ABSTRACT

Aim: Metabolic Stabilization of Bombesin-based Compounds
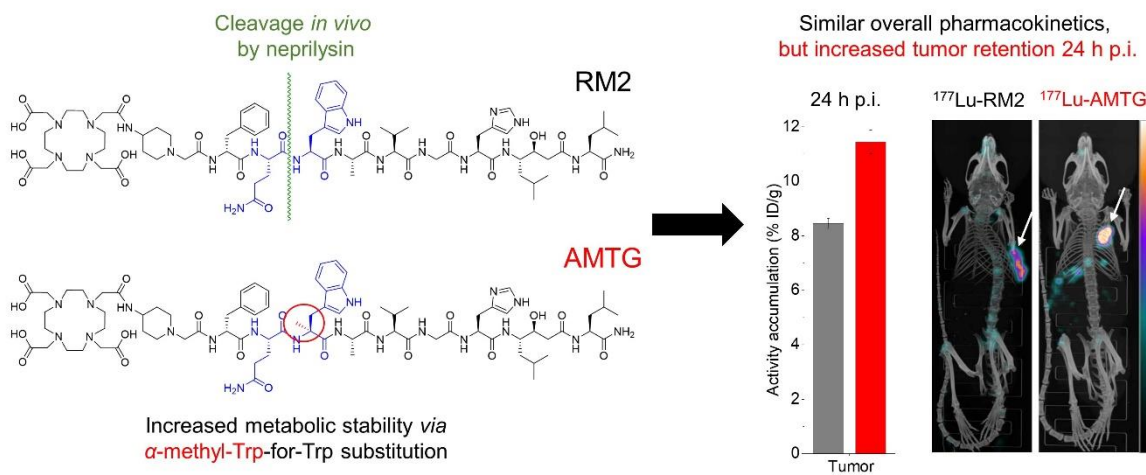
Cleavage *in vivo* by neprilysin

RM2

AMTG

Increased metabolic stability *via* α-methyl-Trp-for-Trp substitution

Similar overall pharmacokinetics, but increased tumor retention 24 h p.i.

24 h p.i.

^{177}Lu-RM2 ^{177}Lu-AMTG

Substitution of L-Trp by *α*-methyl-L-Trp in ^{177}Lu-RM2 results in ^{177}Lu-AMTG, a high affinity GRPR ligand with improved *in vivo* stability

- Supplementary Information -

Thomas Günther[1], Sandra Deiser[1], Veronika Felber[1], Roswitha Beck[1], and Hans-Jürgen Wester[1]

[1]Chair of Pharmaceutical Radiochemistry, Technical University of Munich, Garching, Germany

Corresponding author:

Thomas Günther

Phone: +49.89.289.12203

Technical University of Munich,

Chair of Pharmaceutical Radiochemistry,

Walther-Meissner-Str. 3

85748 Garching

GERMANY

Fax: +49.89.289.12204

E-Mail: thomas.guenther@tum.de

ORCID: https://orcid.org/0000-0002-7412-0297

General Information

The Fmoc-(9-fluorenylmethoxycarbonyl-) and all other protected amino acid analogues were purchased from *Bachem Inc.* (Bubendorf, Switzerland), *Merck KGaA* (Darmstadt, Germany) or *Iris Biotech GmbH* (Marktredwitz, Germany). The *H*-Rink amide ChemMatrix® resin (35-100 mesh particle size, 0.4-0.6 mmol/g loading) was purchased from *Merck KGaA* (Darmstadt, Germany). *CheMatech* (Dijon, France) delivered the chelators DOTA(^{t}Bu)$_3$ as well as DOTAGA(^{t}Bu)$_4$. Peptide syringes were obtained from *VWR International GmbH* (Bruchsal, Germany).

All necessary solvents and other organic reagents were purchased from either, *Alfa Aesar^{TM}* (Karlsruhe, Germany), *Merck KGaA* (Darmstadt, Germany) or *VWR International GmbH* (Bruchsal, Germany). Solid-phase synthesis of the peptides was carried out by manual operation using a Scilogex MX-RL-E Analog Rotisserie Tube Rotator (*Scilogex®*, Rocky Hill, CT, USA). H$_2$O was used after purification by a Barnstead MicroPure system (*Thermo Fisher Scientific Inc.*, Waltham, MA, USA).

Analytical and preparative reversed-phase high performance liquid chromatography (RP-HPLC) were performed using Shimadzu gradient systems (*Shimadzu Deutschland GmbH*, Neufahrn, Germany), each equipped with a SPD-20A UV/Vis detector (220 nm, 254 nm). Different gradients of MeCN (0.1% TFA) in H$_2$O (0.1% TFA) were used as eluents for all RP-HPLC operations.

For analytical measurements, a Nucleosil 100 C18 (125 × 4.6 mm, 5 μm particle size) column (*CS Chromatographie Service GmbH*, Langerwehe, Germany) was used at a flow rate of 1 mL/min. Both, specific gradients and the corresponding retention times t_R as well as the capacity factor *K'* are cited in the text.

Preparative RP-HPLC purification was done with a Multospher 100 RP 18 (250 × 10 mm, 5 μm particle size) column (*CS Chromatographie GmbH*, Langerwehe, Germany) at a constant flow rate of 5 mL/min.

Analytical and preparative radio RP-HPLC was performed using a MultoKrom 100-5 C18 (5 μm, 125 × 4.6 mm) column (*CS Chromatographie GmbH*, Langerwehe, Germany).

Electrospray ionization-mass spectra for characterization of the substances were acquired on an expression[L] CMS mass spectrometer (*Advion Ltd.*, Harlow, UK).

For radiolabeling, ^{177}LuCl$_3$ (Molar Activity (A_M) >3000 GBq/mg, 740 MBq/mL, 0.04 M HCl, *ITG GmbH*, Garching, Germany) was used. Radioactivity was detected through connection of the outlet of the UV-photometer to an AceMate 925-Scint NaI(Tl) well-type scintillation counter from *EG&G Ortec*® (Oak Ridge, TN, USA). Radioactive samples were measured by a WIZARD$^{2®}$ 2480 Automatic γ-Counter (*Perkin Elmer Inc.*, Waltham, MA, USA) and determination of IC_{50} values was carried out using GraphPad Prism 6 (*GraphPad Software Inc.*, San Diego, CA, USA). For radio TLC, a Scan-RAM™ Scanner with Laura™ software (*LabLogic Systems Ltd.*, Broomhill, Sheffield, United Kingdom) was used.

Lyophilization was accomplished using an Alpha 1-2 LDplus lyophilizer (*Martin Christ Gefriertrocknungsanlagen GmbH*, Osterode am Harz, Deutschland) combined with a RZ-2 vacuum pump (*Vacuubrand GmbH & Co KG*, Olching, Germany).

For *in vitro* and *in vivo* studies, the used nutrition mixture Dulbecco's modified eagle's medium/Ham's F-12 (DMEM/F-12, *v/v* = 1/1, with stable glutamine), fetal bovine serum (FBS Superior), phosphate buffered saline (PBS Dulbecco, without Ca^{2+}/Mg^{2+}), trypsin/EDTA (0.05%/0.02% in PBS without Ca^{2+}/Mg^{2+}) solution as well as Hank's balanced salt solution (HBSS, with 0.35 g/L NaHCO$_3$ and Ca^{2+}/Mg^{2+}) were obtained from *Biochrom GmbH* (Berlin, Germany). Solution of purified products was applied using Tracepur® H$_2$O (*Merck KGaA*, Darmstadt, Germany). Bovine serum albumin (BSA) was purchased from *Merck KGaA* (Darmstadt, Germany).

Cells were cultured in CELLSTAR® cell culture flasks and seeded in 24-well plates (*Greiner Bio-One GmbH*, Kremsmünster, Austria) after being counted with a Neubauer hemocytometer (*Paul Marienfeld*, Lauda-Königshofen, Germany) using Trypan Blue (0.4% in 0.81% NaCl and 0.06% potassium phosphate) solution (*Sigma-Aldrich GmbH*, Munich, Germany). Cells were handled inside a MSC Advantage laminar flow cabinet and maintained in a Heracell 150i incubator (*Thermo Fisher Scientific Inc.*, Waltham, MA, USA) at 37 °C in a humidified 5% CO$_2$ atmosphere.

General Procedures (GP) and Execution Protocols

On-resin Peptide Formation (GP1). The respective side-chain protected Fmoc-AA-OH (1.5 eq.) is dissolved in NMP and pre-activated by adding TBTU (1.5 eq.), HOAt (1.5 eq.) and DIPEA (4.5 eq.). After activation for 10 min, the solution is added to resin-bound free amine peptide and shaken for 1.5 h at rt. Subsequently, the resin is washed with NMP (6 × 20 mL/g resin) and after Fmoc deprotection (GP2), the next amino acid is coupled analogously.

On-resin Fmoc Deprotection (GP2). The resin-bound Fmoc-peptide is treated with 20% piperidine in NMP (*v/v*) for 5 min and subsequently for 15 min. Afterwards, the resin is washed with NMP (6 × 20 mL/g resin).

Conjugation of Chelator (GP3). The protected chelator DOTA(^{t}Bu)$_3$ or DOTAGA(^{t}Bu)$_4$ (1.5 eq.) is dissolved in NMP and pre-activated by adding TBTU (1.5 eq.), HOAt (1.5 eq.) and DIPEA (4.5 eq.). After activation for 10 min, the solution is added to resin-bound *N*-terminal deprotected peptide (1.0 eq.) and shaken for 3 h at rt. Subsequently, the resin is washed with NMP (3 × 20 mL/g resin) and DCM (3 × 20 mL/g resin).

Peptide Cleavage from the Resin with additional Deprotection of acid labile Protecting Groups (GP4). The fully protected resin-bound peptide is washed with DCM, afterwards dissolved in a mixture of TFA/TIPS/DCM (*v/v/v*; 95/2.5/2.5) and shaken for 45 min. The solution is filtered off and the resin is treated in the same way for another 45 min. Both filtrates are combined and concentrated under a stream of nitrogen. After dissolving the residue in MeOH and precipitation in diethyl ether, the liquid is decanted and the remaining solid is dried. As the deprotection of the ^{t}Bu groups is usually not complete using this procedure (see Supplemental Fig. 11 for AMTG as an example), a further deprotection method is used (GP5).

Complete Deprotection of ^{t}Bu (GP5). Removal of remaining ^{t}Bu protecting groups after peptide cleavage from the resin (GP4) is carried out by dissolving the crude DOTA or DOTAGA coupled product in TFA and stirring for 6 h and 16 h at rt, respectively. After removing TFA under a stream of nitrogen, the crude unprotected product is obtained.

Cold Complexation

The purified chelator-containing ligand (10^{-3} M in Tracepur® H$_2$O, *Merck KGaA*, Darmstadt, Germany, 1.0 eq.) and ^{nat}LuCl$_3$ (20 mM in Tracepur® H$_2$O, 2.5 eq.) were diluted with Tracepur® H$_2$O to a final concentration of 10^{-4} M and heated to 95 °C for 30 min. After cooling to room temperature, the crude product was obtained and used without further purification for IC_{50} studies. In order to confirm that the remaining excess of 1.5 eq. ^{nat}LuCl$_3$ did not affect the cell-based assay, a validation experiment was carried out (see *In Vitro Experiments* below).

Radiolabeling

^{125}I-Labeling. Briefly, 0.2 mg of D-Tyr^6-MJ9 were dissolved in 20 µL Tracepur® H$_2$O and 280 µL TRIS buffer (25 mM TRIS · HCl, 0.4 M NaCl, pH = 7.9). After solution was transferred to a vial containing 150 µg surface-bound Iodo-Gen® (1,3,4,6-Tetrachloro-3α,6α-diphenylglycouril, *Merck KGaA*, Darmstadt, Germany), 5.0 µL (16 MBq) ^{125}I-NaI (74 TBq/mmol, 3.1 GBq/mL, 40 mM NaOH, *Hartmann Analytic*, Braunschweig, Germany) were added. The reaction solution was incubated for 15 min at room temperature and purified by RP-HPLC. Immediately after purification, sodium ascorbate (0.1 M in Tracepur® H$_2$O, 10 vol-%) was added to prevent radiolysis.
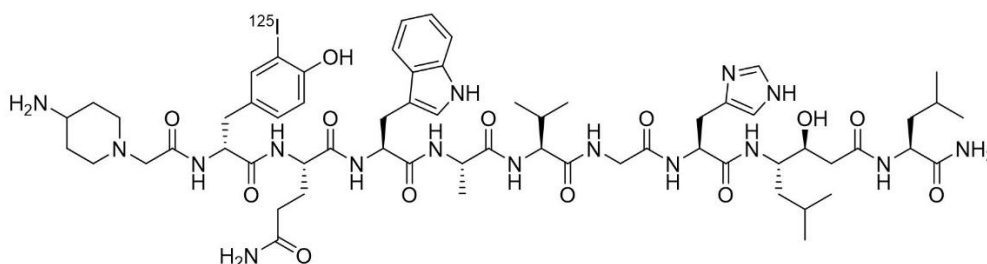
SUPPLEMENTAL FIGURE 1. Structural formula of the radiolabeled reference 3-^{125}I-D-Tyr^6-MJ9.

3-^{125}I-D-Tyr^6-MJ9. RP-HPLC (20→35% MeCN in 20 min). t_R = 18.5 min, K' = 12.21.

3-I-D-Tyr^6-MJ9. RP-HPLC (20→35% MeCN in 20 min). t_R = 18.4 min, K' = 12.14.

Calculated monoisotopic mass (C$_{78}$H$_{118}$N$_{20}$O$_{19}$): 1394.6, found: m/z = 698.3 [M+2H]$^{2+}$, 1394.9 [M+H]$^+$.
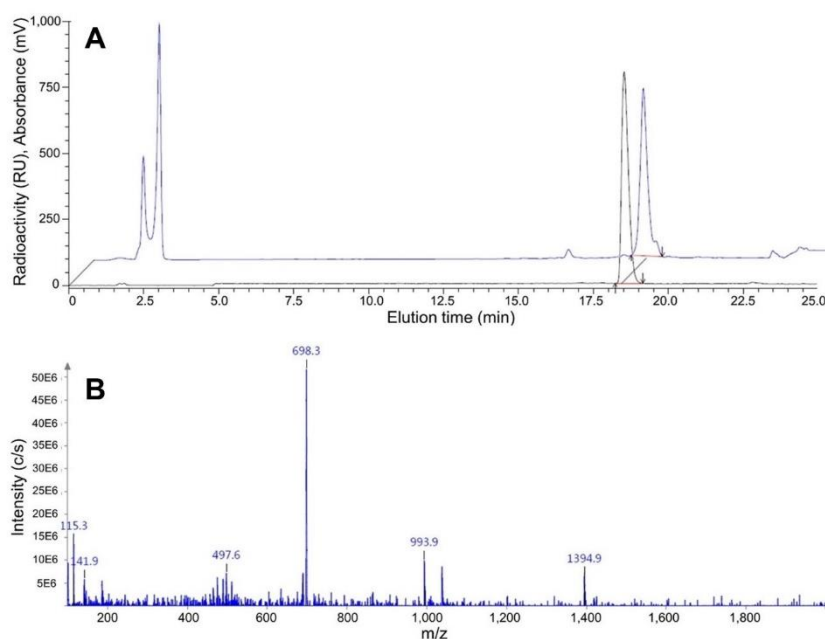
SUPPLEMENTAL FIGURE 2. (A) Confirmation of peptide integrity for 3-^{125}I-D-Tyr^6-MJ9 (black), as analyzed by analytical (radio-)RP-HPLC (MultoKrom 100-5 C18, 5 µm, 125 × 4.6 mm, *CS Chromatographie GmbH*, Langerwehe, Germany; 20→35% MeCN in H$_2$O + 0.1% TFA in 20 min) *via* co-injection of the cold ligand (blue). (B) Mass spectrum of 3-I-D-Tyr^6-MJ9.

^{177}Lu-Labeling. A solution of the purified chelator-containing ligand (10^{-3} M in Tracepur$^®$ H$_2$O, 1 µL), NaOAc buffer (1.0 M, pH = 5.50, 10 µL) and approximately 10-30 MBq ^{177}LuCl$_3$ (0.04 M in HCl) were diluted with HCl (0.04 M) to a total volume of 90 µL and heated to 95 °C for 10 min. Immediately after labeling, sodium ascorbate (0.1 M, 10 µL) was added to prevent radiolysis. Incorporation of ^{177}Lu was determined by radio TLC (ITLC-SG chromatography paper, mobile phase: 0.1 M trisodium citrate). Radiochemical purity of the labeled compound was determined by radio RP-HPLC.

Characterization of RM2 Derivatives and NeoBOMB1

All mentioned compounds based on the core structure of RM2 were synthesized by standard Fmoc-based SPPS (**GP1**-**5**) using a *H*-Rink amide ChemMatrix$^®$ resin (35-100 mesh particle size, 0.4-0.6 mmol/g loading, *Merck KGaA*, Darmstadt, Germany). After finishing the peptide sequence with slightly modifications within the RM2 sequence, a chelator was coupled

at the resin (**GP3**). Thereafter, the peptide was cleaved (**GP4**) and furthermore, remaining acid labile protection groups were deprotected by TFA (**GP5**) and purified by RP-HPLC.

RM2 (DOTA-Pip-D-Phe-Gln-Trp-Ala-Val-Gly-His-Sta-Leu-NH₂)
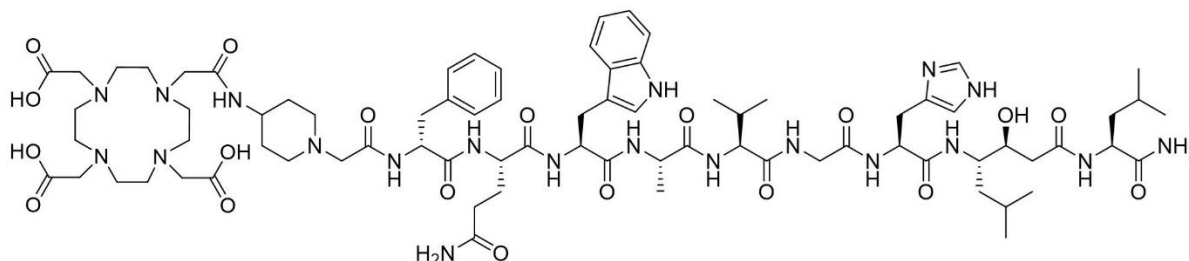
SUPPLEMENTAL FIGURE 3.   Structural formula of the parent compound RM2.

RM2. RP-HPLC (10→90% MeCN in 15 min): t_R = 6.8 min, K' = 3.25.

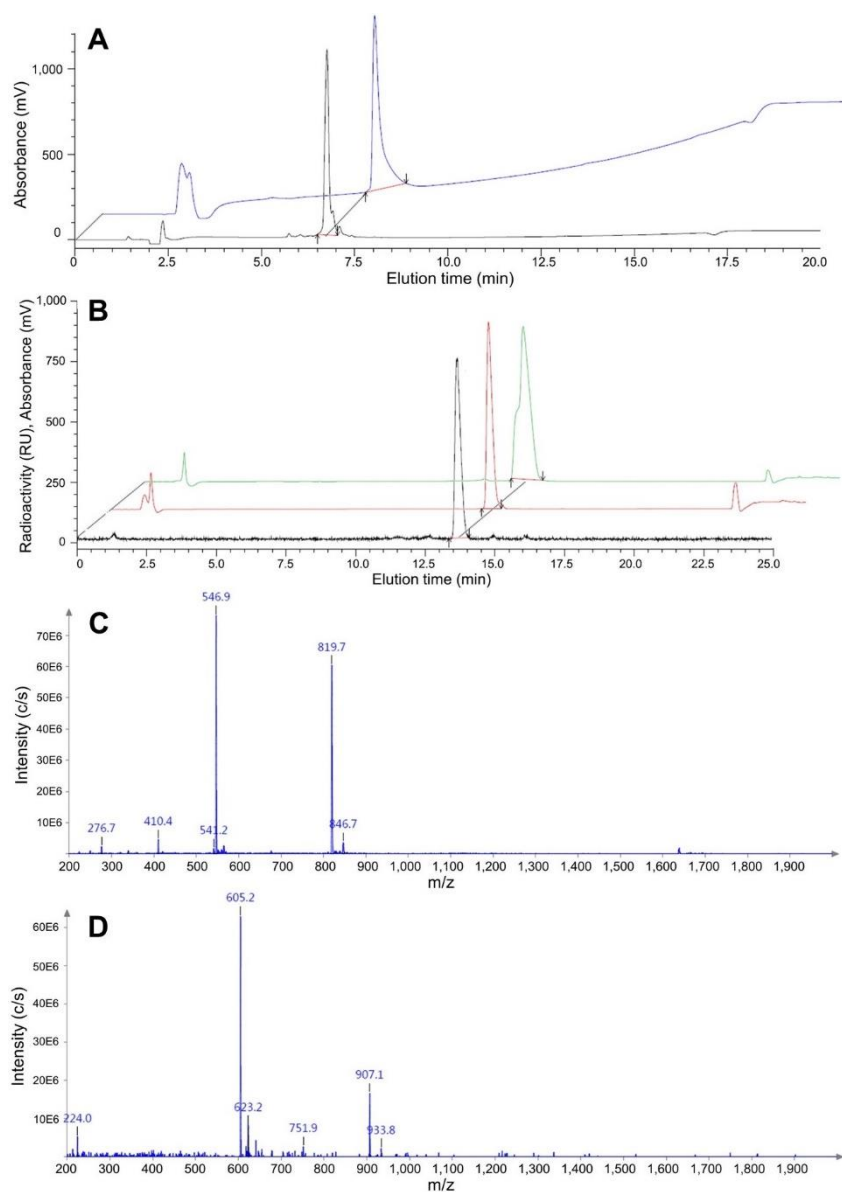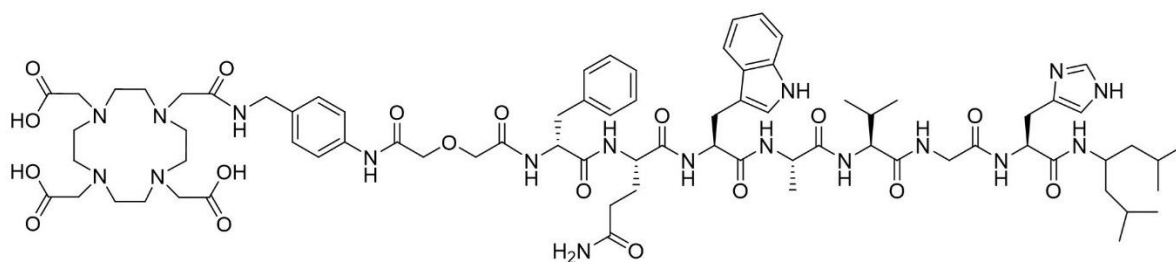RP-HPLC (20→35% MeCN in 15 min): t_R = 13.6 min, K' = 9.46.

Calculated monoisotopic mass ($C_{78}H_{118}N_{20}O_{19}$): 1638.9, found: m/z = 546.9 $[M+3H]^{3+}$, 819.7 $[M+2H]^{2+}$.

^{nat}Lu-*RM2.* RP-HPLC (10→90% MeCN in 15 min): t_R = 7.3 min, K' = 2.65.

RP-HPLC (20→35% MeCN in 15 min): t_R = 13.6 min, K' = 9.46.

Calculated monoisotopic mass ($C_{78}H_{115}LuN_{20}O_{19}$): 1810.8, found: m/z = 605.2 $[M+3H]^{3+}$, 907.1 $[M+2H]^{2+}$.

SUPPLEMENTAL FIGURE 4. (A) Confirmation of peptide identity and integrity for RM2 (black) and natLu-RM2 (blue), as analyzed by analytical RP-HPLC (MultoKrom 100-5 C18, 5 µm, 125 × 4.6 mm, *CS Chromatographie GmbH*, Langerwehe, Germany; 10→90% MeCN in H_2O + 0.1% TFA in 15 min). (B) Confirmation of peptide identity and integrity for ^{177}Lu-RM2 (black), natLu-RM2 (red) and RM2 (green), as analyzed by analytical (radio-)RP-HPLC (MultoKrom 100-5 C18, 5 µm, 125 × 4.6 mm, *CS Chromatographie GmbH*, Langerwehe, Germany; 20→35% MeCN in H_2O + 0.1% TFA in 20 min). Mass spectra of (C) RM2 and (D) natLu-RM2.

NeoBOMB1 (DOTA-pABzA-DIG-D-Phe-Gln-Trp-Ala-Val-Gly-His-NH-CH[CH₂-CH(CH₃)₂]₂)

SUPPLEMENTAL FIGURE 5. Structural formula of the second reference compound NeoBOMB1.

NeoBOMB1. RP-HPLC (10→90% MeCN in 15 min): t_R = 9.5 min, K' = 3.75.

RP-HPLC (20→35% MeCN in 15 min): t_R = 22.4 min, K' = 16.23.

Calculated monoisotopic mass ($C_{77}H_{110}N_{18}O_{18}$): 1574.8, found: m/z = 787.7 $[M+2H]^{2+}$, 1574.6 $[M+H]^+$.

*natLu-NeoBOMB1.* RP-HPLC (10→90% MeCN in 15 min): t_R = 9.7 min, K' = 3.85.

RP-HPLC (20→35% MeCN in 15 min): t_R = 22.4 min, K' = 16.23.

Calculated monoisotopic mass ($C_{77}H_{107}LuN_{18}O_{18}$): 1746.7, found: m/z = 583.5 $[M+3H]^{3+}$, 874.8 $[M+2H]^{2+}$.
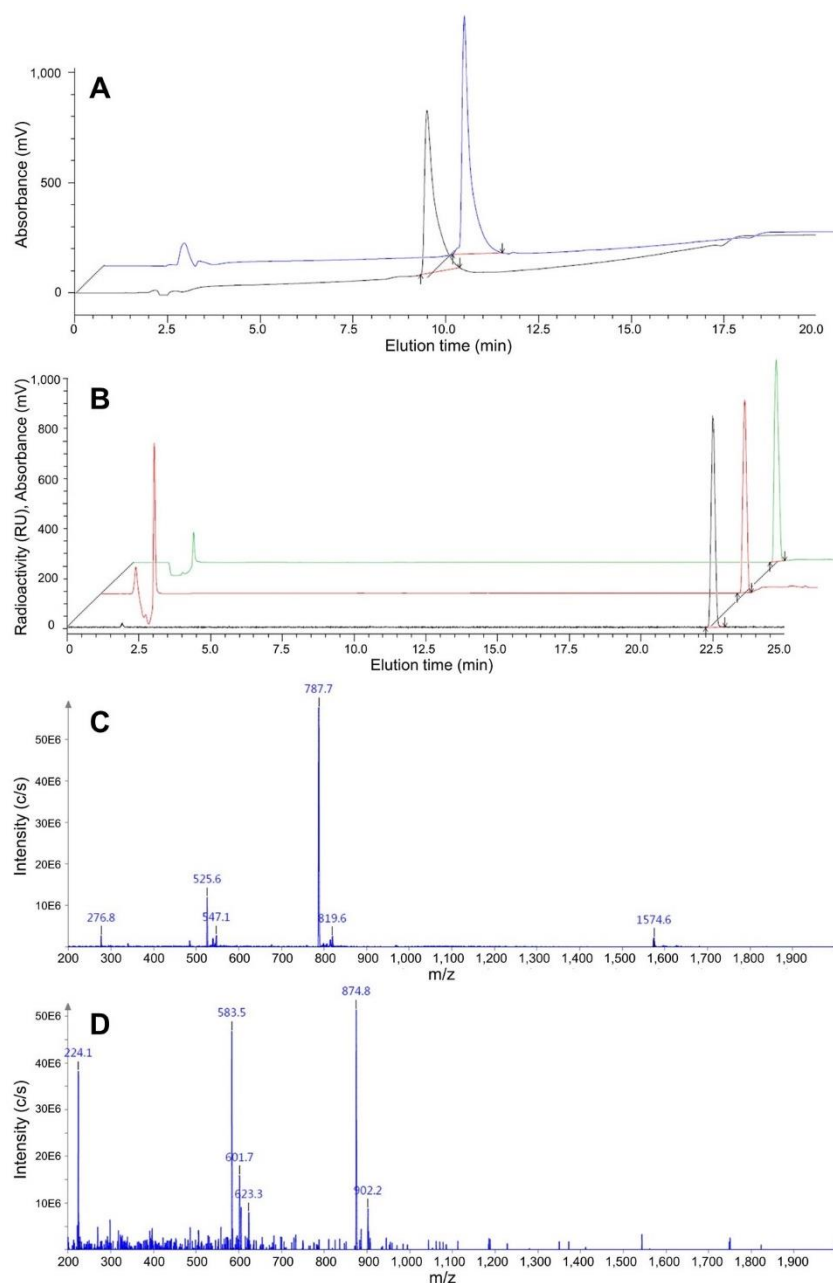
SUPPLEMENTAL FIGURE 6. (A) Confirmation of peptide identity and integrity for NeoBOMB1 (black) and natLu-NeoBOMB1 (blue), as analyzed by analytical RP-HPLC (MultoKrom 100-5 C18, 5 µm, 125 × 4.6 mm, *CS Chromatographie GmbH*, Langerwehe, Germany; 10→90% MeCN in H_2O + 0.1% TFA in 15 min). (B) Confirmation of peptide identity and integrity for ^{177}Lu-NeoBOMB1 (black), natLu-NeoBOMB1 (red) and NeoBOMB1 (green), as analyzed by analytical (radio-)RP-HPLC (MultoKrom 100-5 C18, 5 µm, 125 × 4.6 mm, *CS Chromatographie GmbH*, Langerwehe, Germany; 20→35% MeCN in H_2O + 0.1% TFA in 20 min). Mass spectra of (C) NeoBOMB1 and (D) natLu-NeoBOMB1.

AMTG (DOTA-Pip-D-Phe-Gln-*α*-Me-Trp-Ala-Val-Gly-His-Sta-Leu-NH₂)
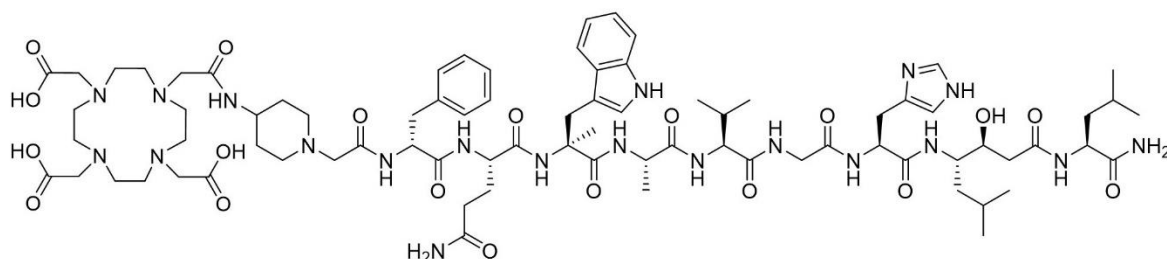
SUPPLEMENTAL FIGURE 7. Structural formula of AMTG.

AMTG. RP-HPLC (10→90% MeCN in 15 min): t_R = 7.5 min, K' = 2.75.

RP-HPLC (20→35% MeCN in 15 min): t_R = 15.2 min, K' = 10.69.

Calculated monoisotopic mass ($C_{79}H_{120}N_{20}O_{19}$): 1652.9, found: m/z = 551.6 $[M+3H]^{3+}$, 826.6 $[M+2H]^{2+}$, 1652.7 $[M+H]^+$.

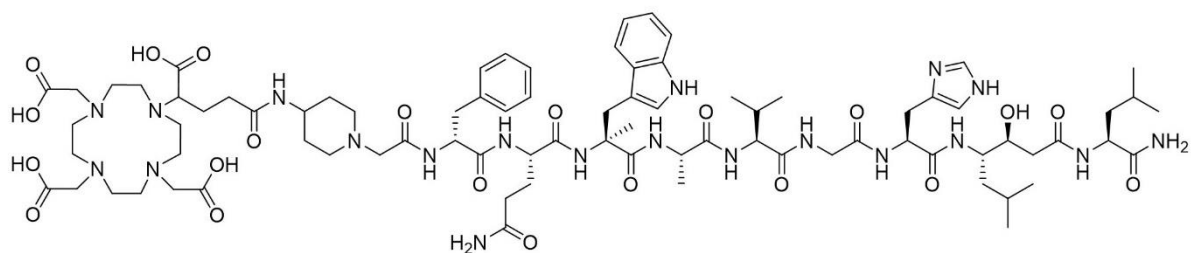*natLu-AMTG.* RP-HPLC (10→90% MeCN in 15 min): t_R = 7.5 min, K' = 2.75.

RP-HPLC (20→35% MeCN in 15 min): t_R = 15.0 min, K' = 10.54.

Calculated monoisotopic mass ($C_{79}H_{117}LuN_{20}O_{19}$): 1824.8, found: m/z = 609.6 $[M+3H]^{3+}$, 914.0 $[M+2H]^{2+}$.
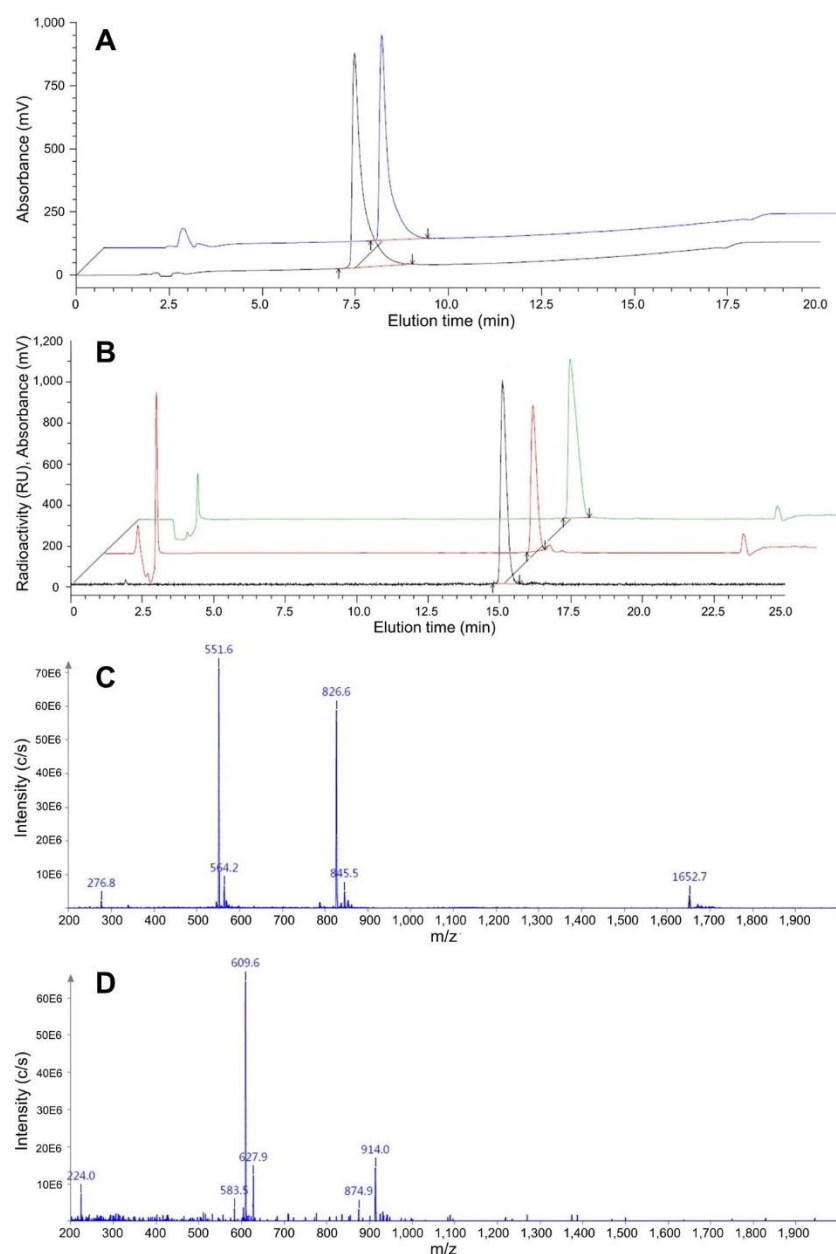
SUPPLEMENTAL FIGURE 8. (A) Confirmation of peptide identity and integrity for AMTG (black) and natLu-AMTG (blue), as analyzed by analytical RP-HPLC (MultoKrom 100-5 C18, 5 μm, 125 × 4.6 mm, *CS Chromatographie GmbH*, Langerwehe, Germany; 10→90% MeCN in H_2O + 0.1% TFA in 15 min). (B) Confirmation of peptide identity and integrity for ^{177}Lu-AMTG (black), natLu-AMTG (red) and AMTG (green), as analyzed by analytical (radio-)RP-HPLC (MultoKrom 100-5 C18, 5 μm, 125 × 4.6 mm, *CS Chromatographie GmbH*, Langerwehe, Germany; 20→35% MeCN in H_2O + 0.1% TFA in 20 min). Mass spectra of (C) AMTG and (D) natLu-AMTG.

AMTG2 (DOTAGA-Pip-D-Phe-Gln-α-Me-Trp-Ala-Val-Gly-His-Sta-Leu-NH₂)

SUPPLEMENTAL FIGURE 9.   Structural formula of AMTG2.

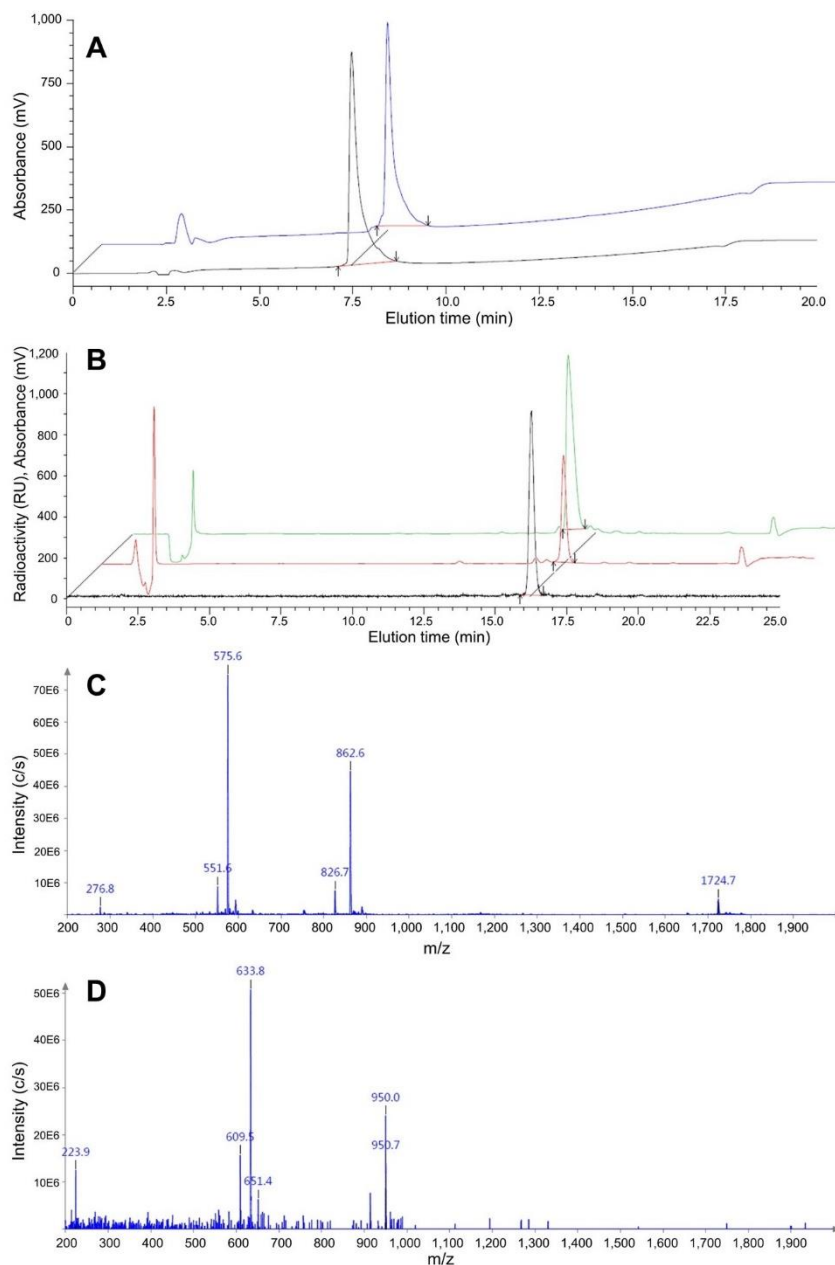*AMTG2.* RP-HPLC (10→90% MeCN in 15 min): t_R = 7.5 min, $K^{'}$ = 2.75.

RP-HPLC (20→35% MeCN in 15 min): t_R = 15.2 min, $K^{'}$ = 10.69.

Calculated monoisotopic mass ($C_{82}H_{124}N_{20}O_{21}$): 1724.9, found: m/z = 575.6 [M+3H]$^{3+}$, 862.6 [M+2H]$^{2+}$, 1724.7 [M+H]$^{+}$.

[nat]Lu-AMTG2. RP-HPLC (10→90% MeCN in 15 min): t_R = 7.7 min, $K^{'}$ = 2.85.

RP-HPLC (20→35% MeCN in 15 min): t_R = 16.2 min, $K^{'}$ = 11.46.

Calculated monoisotopic mass ($C_{82}H_{121}LuN_{20}O_{21}$): 1896.8, found: m/z = 633.8 [M+3H]$^{3+}$, 950.0 [M+2H]$^{2+}$.

SUPPLEMENTAL FIGURE 10. (A) Confirmation of peptide identity and integrity for AMTG2 (black) and natLu-AMTG2 (blue), as analyzed by analytical RP-HPLC (MultoKrom 100-5 C18, 5 µm, 125 × 4.6 mm, *CS Chromatographie GmbH*, Langerwehe, Germany; 10→90% MeCN in H_2O + 0.1% TFA in 15 min). (B) Confirmation of peptide identity and integrity for ^{177}Lu-AMTG2 (black), natLu-AMTG2 (red) and AMTG2 (green), as analyzed by analytical (radio-)RP-HPLC (MultoKrom 100-5 C18, 5 µm, 125 × 4.6 mm, *CS Chromatographie GmbH*, Langerwehe, Germany; 20→35% MeCN in H_2O + 0.1% TFA in 20 min). Mass spectra of (C) AMTG2 and (D) natLu-AMTG2.
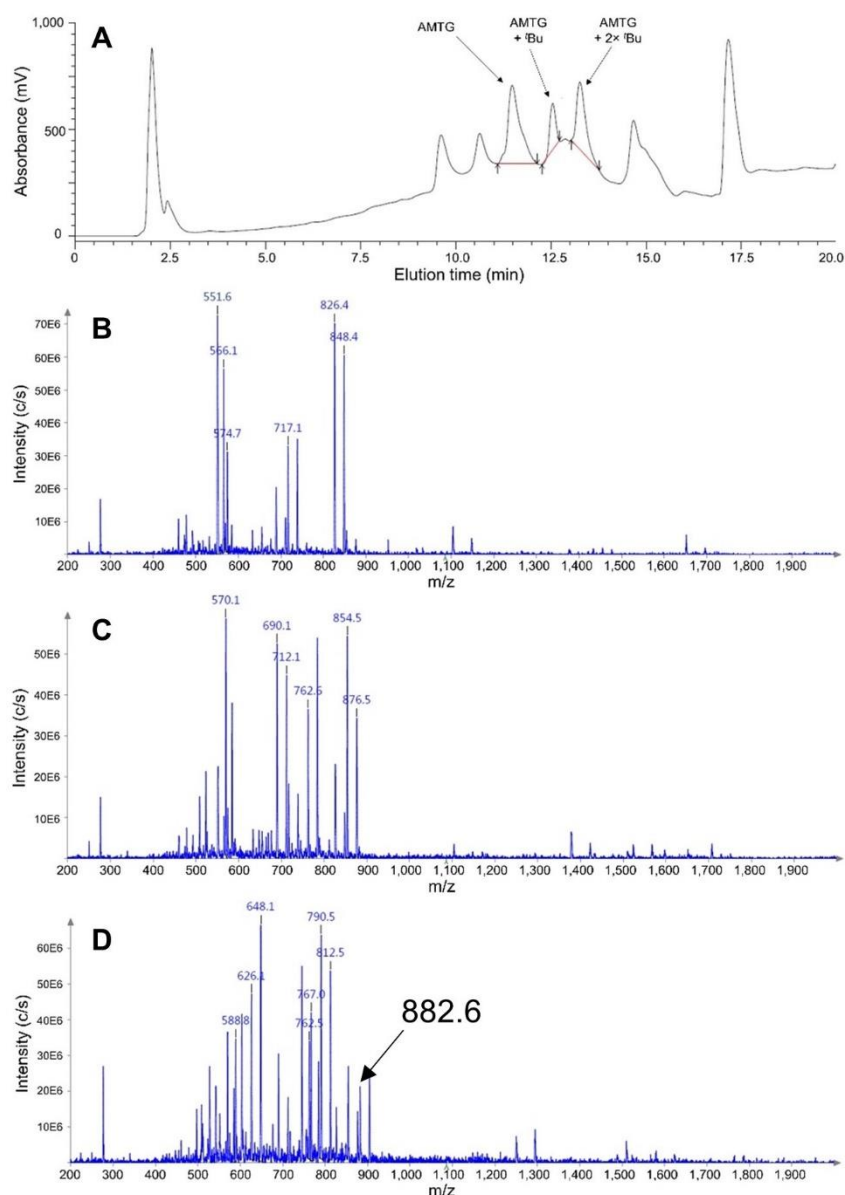
SUPPLEMENTAL FIGURE 11. Incomplete deprotection of *t*Bu groups of the DOTA moiety in AMTG (calculated monoisotopic mass: 1652.9), as analyzed by (A) analytical RP-HPLC (MultoKrom 100-5 C18, 5 µm, 125 × 4.6 mm, *CS Chromatographie GmbH*, Langerwehe, Germany; 20→35% MeCN in H_2O + 0.1% TFA in 15 min) and mass spectrometry (B-D). (B) Mass spectrum of the fully deprotected compound (AMTG: $K' = 6.2$, t_R = 11.5 min, mass found: m/z = 826.4 $[M+2H]^{2+}$). (C) Mass spectrum of the compound carrying one *t*Bu group (AMTG + *t*Bu: $K' = 6.8$, t_R = 12.5 min, mass found: m/z = 854.5 $[M+2H]^{2+}$). (D) Mass spectrum of the compound carrying two *t*Bu groups (AMTG + 2× *t*Bu: $K' = 7.3$, t_R = 13.2 min, mass found: m/z = 882.6 $[M+2H]^{2+}$).
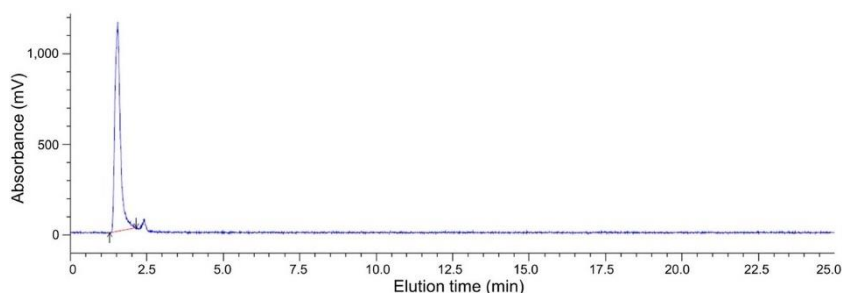
SUPPLEMENTAL FIGURE 12. Chromatogram of ^{177}Lu-LuCl$_3$, (elution time t_R = 1.54 min) as analyzed by analytical radio-RP-HPLC (MultoKrom 100-5 C18, 5 µm, 125 × 4.6 mm, *CS Chromatographie GmbH*, Langerwehe, Germany; 20→35% MeCN in H$_2$O + 0.1% TFA in 20 min).

In Vitro Experiments

Cell Culture. GRPR$^+$ PC-3 cells (*Merck KGaA*, Darmstadt, Germany) were cultivated in Dulbecco's modified eagle's medium/Ham's F-12 (DMEM/F-12, *v/v* = 1/1, with stable glutamine, *Biochrom GmbH*, Berlin, Germany) supplemented with fetal bovine serum (10%, FBS Superior, *Biochrom GmbH*, Berlin, Germany) at 37 °C in a humidified 5% CO$_2$ atmosphere. GRPR$^+$ T-47D cells (*American Type Culture Collection*, Manassas, VA, USA) were cultivated in Gibco™ RPMI 1640 Medium (*Fisher Scientific GmbH*, Schwerte, Germany) supplemented with fetal bovine serum (10%, FBS Superior, *Biochrom GmbH*, Berlin, Germany) at 37 °C in a humidified 5% CO$_2$ atmosphere. A mixture of trypsin and ethylenediaminetetraacetic acid (0.05%, 0.02%) in PBS (*Biochrom GmbH*, Berlin, Germany) was used in order to harvest cells. Cells were counted with a Neubauer hemocytometer (*Paul Marienfeld*, Lauda-Königshofen, Germany).

Determination of IC$_{50}$. For determination of the GRPR affinity on both PC-3 and T-47D cells (*IC$_{50}$*), cells were harvested 24 ± 2 h before the experiment and seeded in 24-well plates (1.5 × 10^5 cells in 1 mL/well).

After removal of the culture medium, the cells were washed once with 500 µL of HBSS (Hank's balanced salt solution, *Biochrom GmbH*, Berlin, Germany, with addition of 1% bovine serum albumin (BSA, *v/v*)) and left in 200 µL HBSS (1% BSA, *v/v*) for 9 min at room temperature for equilibration. Next, 25 µL per well of solutions, containing either HBSS (1%

BSA, *v/v*) as control or the respective compound in increasing concentration (10^{-10}–10^{-4} M in HBSS (1% BSA, *v/v*)), were added with subsequent addition of 25 µL of 3-^{125}I-D-Tyr^6-MJ9 (2.0 nM) in HBSS (1% BSA, *v/v*).

All experiments were performed in triplicate for each concentration. After 2 h incubation at rt, the experiment was terminated by removal of the medium and consecutive rinsing with 300 µL of HBSS (1% BSA, *v/v*). The media of both steps were combined in one fraction and represent the amount of free 3-^{125}I-D-Tyr^6-MJ9. Afterwards, the cells were lysed with 300 µL of 1 M NaOH for at least 15 min and united with the 300 µL NaOH of the following washing step. Quantification of bound and free 3-^{125}I-D-Tyr^6-MJ9 was accomplished in a *γ*-counter. *IC*$_{50}$ determination for each conjugate was repeated twice.

Brief Competition Study to validate Assay Conditions. In order to exclude an impact of free ^{nat}LuCl$_3$ (from labeling procedure, see *Cold Complexation* above) in the above-described *IC*$_{50}$ assay, the study was repeated for ^{nat}Lu-AMTG applying the same conditions. However, in addition to the used dilution series (10^{-10}–10^{-4} M in HBSS (1% BSA, *v/v*)) of ^{nat}Lu-AMTG (1.5-fold excess of free ^{nat}Lu^{3+} present), two further dilution series were prepared. On the one hand, a 1,500-fold and on the other hand, a 1.5×10^6-fold excess of free ^{nat}Lu^{3+} was added to each dilution of ^{nat}Lu-AMTG.

The study confirmed that no noticeable effect of free ^{nat}Lu^{3+} on the cellular uptake or displacement of 3-^{125}I-D-Tyr^6-MJ9 and thus *IC*$_{50}$ values in the above-described assay could be determined (Supplemental Fig. 13).
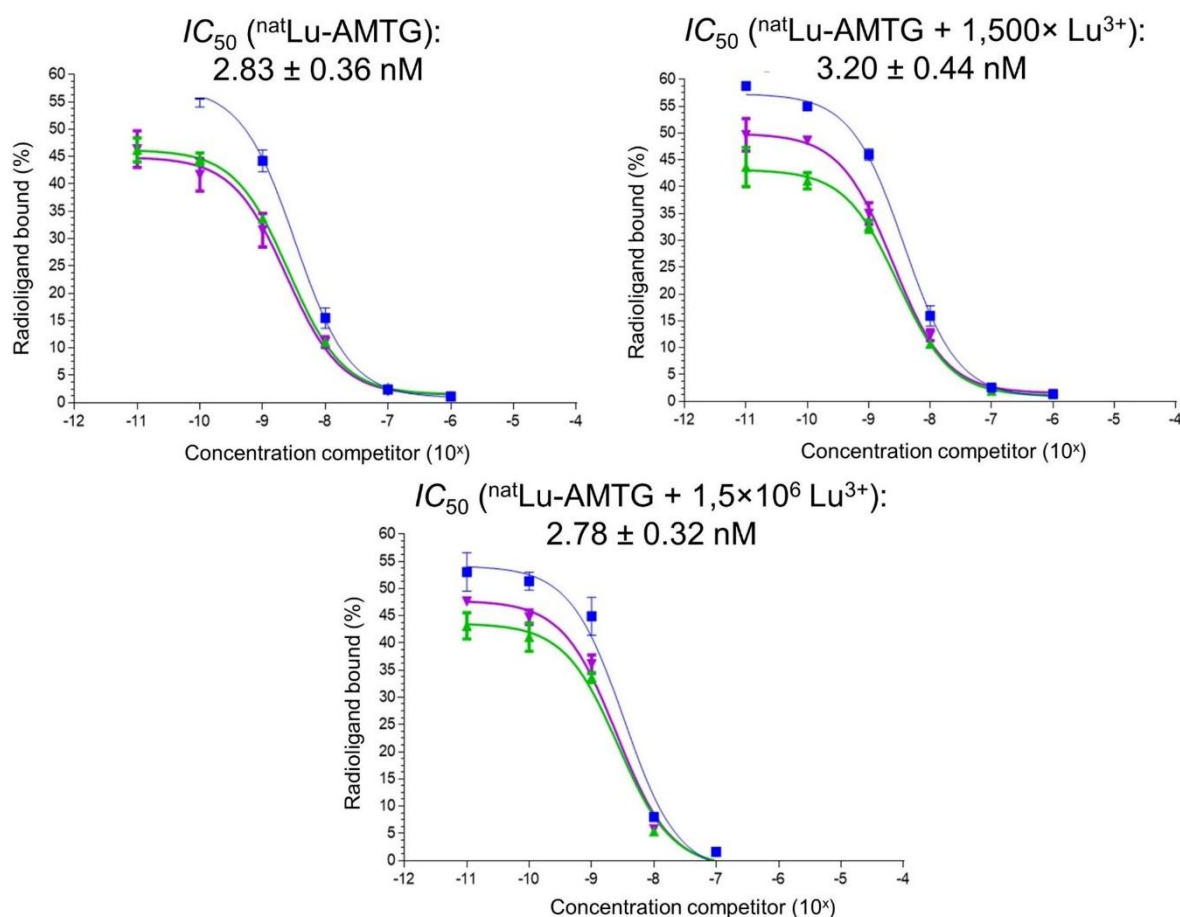
SUPPLEMENTAL FIGURE 13. Sigmoidal binding curves and calculated mean IC_{50}´s as obtained by competitive binding studies of ^{nat}Lu-AMTG, ^{nat}Lu-AMTG with a 1,500-fold excess of free Lu^{3+} and ^{nat}Lu-AMTG with a 1.5×10^6-fold excess of free Lu^{3+}. Binding studies have been carried out in triplicate, using 1.5×10^5 PC-3 cells/ml/well, rt, 2 h; using 3-^{125}I-D-Tyr^6-MJ9 (0.2 nM/well) as radiolabeled reference (n = 3).

Receptor-mediated Internalization. For internalization studies, PC-3 cells were harvested 24 ± 2 h before the experiment and seeded in poly-L-lysine coated 24-well plates (1.5×10^5 cells/well, 1 mL, *Greiner Bio-One*, Kremsmünster, Austria). Subsequent to the removal of the culture medium, the cells were washed once with 500 µL DMEM/F-12 (5% BSA, *v/v*) and left to equilibrate at 37 °C for at least 15 min in 200 µL DMEM/F-12 (5% BSA, *v/v*). Each well was treated with either 25 µL of DMEM/F-12 (5% BSA, *v/v*) or 25 µL ^{nat}Lu-RM2 (10^{-3} M) for blockade. Next, 25 µL of the ^{177}Lu-labeled GRPR analogue (10 nM) was added and the cells were incubated at 37 °C for 60 min.

The experiment was terminated by placing the 24-well plate on ice for 1 min and consecutive removal of the medium. Each well was rinsed with 300 µL ice-cold PBS and the fractions from these first two steps were combined, representing the amount of free 3-^{125}I-D-Tyr^6-MJ9. Removal of surface bound activity was accomplished by incubation of the cells with 300 µL of ice-cold Acid Wash solution (0.02 M NaOAc, pH = 5.0) for 10 min at room temperature and rinsed again with 300 µL of ice-cold PBS. The internalized activity was determined by incubation of the cells in 300 µL NaOH (1 M) and the combination with the fraction of a subsequent washing step with 300 µL NaOH (1 M).

Each experiment (control and blockade) was performed sixfold. Free, surface bound and internalized activity was quantified in a γ-counter. Data was corrected for non-specific internalization.

In Vivo Experiments

Establishment of Tumor Xenografts. PC-3 cells (5.0 × 10^6 cells per 200 µL) were suspended in a mixture ($v/v = 1/1$) of Dulbecco's modified eagle's medium/Ham's F-12 (DMEM/F-12) with Glutamax-I (1/1) and Cultrex$^®$ Basement Membrane Matrix Type 3 (*Trevigen Inc.*, Gaithersburg, MD, USA) and inoculated subcutaneously onto the right shoulder of 6–10 weeks old female CB17-SCID mice (*Charles River Laboratories International Inc.*, Sulzfeld, Germany). Mice were used for experiments when tumor volume was 125-500 mm^3 (2–3 weeks after inoculation).
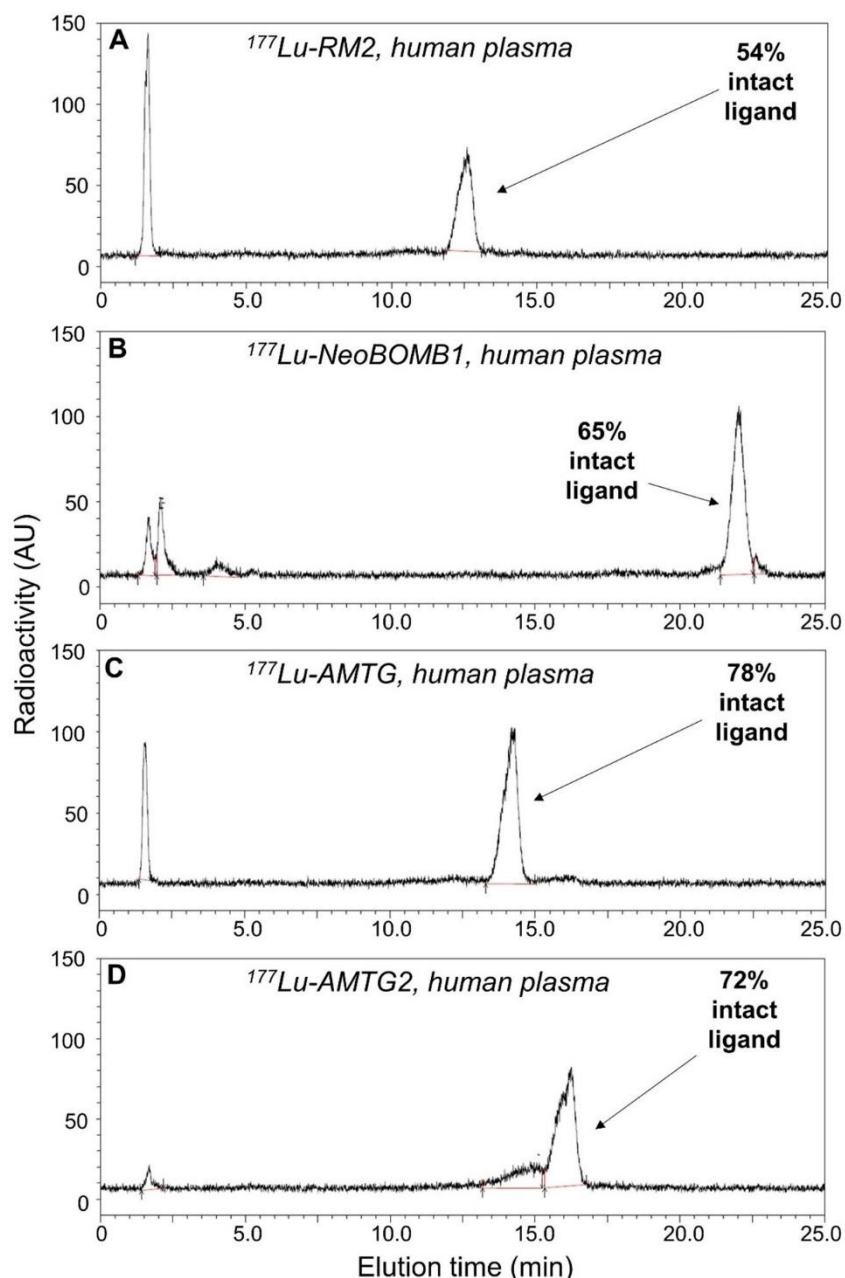
Supplemental Data

SUPPLEMENTAL TABLE 1. Preclinical data of ^{nat}Lu-RM2, ^{nat}Lu-NeoBOMBM1, ^{nat}Lu-AMTG and ^{nat}Lu-AMTG2. Affinity data were determined on PC-3 and T-47D cells (1.5 × 10^5 cells/well) and 3-^{125}I-D-Tyr^6-MJ9 (c = 0.2 nM) as radiolabeled reference (2 h, rt, HBSS + 1% BSA, *v/v*). Receptor-mediated internalization (0.25 pmol/well) was determined on PC-3 cells as percent (%) of the applied activity after incubation for 1 h (37 °C, DMEM/F-12 + 5% BSA (*v/v*), 1.5 × 10^5 cells/well). Data are corrected for non-specific binding (10^{-3} M ^{nat}Lu-RM2). Metabolic stability *in vitro* was determined in human plasma by incubation at 37 °C for 72 ± 2 h (n = 4). Metabolic stability *in vivo* was determined on CB17-SCID mice at 30 min p.i. (n = 3). Data are expressed as mean ± SD. Metabolic stability of the ^{177}Lu-RM2 derivatives as determined *in vitro* and *in vivo*. * ^{nat}Lu-labeled, ** ^{177}Lu-labeled.

	IC_{50} (nM)		GRPR-mediated internalization (%)	$\log D_{7.4}$	Fraction intact tracer (%)		
GRPR-targeted compound	PC-3 cells (n = 3)*	T-47D-cells (n = 3)*	(n = 5)**	(n = 6)**	human plasma, *in vitro* at 72 ± 2 h (n = 4)**	murine blood, *in vivo* at 30 min p.i. (n = 3)**	murine urine, *in vivo* at 30 min p.i. (n = 3)**
RM2	3.5 ± 0.2	1.2 ± 0.2	2.92 ± 0.20	−2.51 ± 0.02	38.7 ± 9.3	11.4 ± 3.7	0.5 ± 0.1
NeoBOMB1	4.2 ± 0.1	1.1 ± 0.2	13.91 ± 0.64	−0.57 ± 0.03	61.9 ± 2.1	75.9 ± 0.6	3.9 ± 1.3
AMTG	3.0 ± 0.1	1.0 ± 0.1	3.03 ± 0.18	−2.28 ± 0.06	77.7 ± 8.7	92.9 ± 0.7	68.2 ± 3.1
AMTG2	4.7 ± 0.2	4.6 ± 0.2	5.88 ± 0.33	−2.51 ± 0.11	66.2 ± 5.1	77.6 ± 3.1	61.6 ± 1.6

SUPPLEMENTAL TABLE 2. Tumor/background ratios of ^{177}Lu-RM2 and its analogues as well as ^{177}Lu-NeoBOMB1 for the selected organs of PC-3 tumor-bearing CB17-SCID mice at 24 h p.i. (n = 4).

| Organ	^{177}Lu-RM2	^{177}Lu-AMTG	^{177}Lu-AMTG2	^{177}Lu-NeoBOMB1
Blood	688.7 ± 79.4	2702.0 ± 321.0	723.1 ± 109.2	175.5 ± 100.2
Heart	152.8 ± 7.4	575.3 ± 98.3	646.9 ± 597.4	87.5 ± 37.0
Lung	91.4 ± 16.4	357.2 ± 107.8	181.2 ± 29.6	16.7 ± 2.0
Liver	18.8 ± 1.3	85.3 ± 19.5	27.4 ± 6.4	5.6 ± 2.7
Spleen	42.8 ± 5.2	114.3 ± 24.9	59.4 ± 14.2	5.3 ± 3.1
Pancreas	19.9 ± 2.5	26.1 ± 12.0	8.4 ± 0.8	0.9 ± 0.2
Stomach	50.8 ± 19.3	128.3 ± 47.7	64.9 ± 5.0	5.6 ± 0.2
Intestine	39.7 ± 7.0	80.0 ± 49.7	27.5 ± 5.7	8.5 ± 0.6
Kidney	4.7 ± 0.1	10.5 ± 2.5	4.3 ± 0.4	4.7 ± 2.3
Adrenal	10.9 ± 1.7	34.3 ± 21.8	22.7 ± 2.9	2.1 ± 0.1
Muscle	1680.2 ± 978.9	2247.8 ± 687.3	4133.8 ± 2593.0	1017.0 ± 598.5
Bone	7.9 ± 3.6	234.3 ± 69.4	37.9 ± 11.3	42.2 ± 17.4

SUPPLEMENTAL FIGURE 14. *In vitro* stability of ^{177}Lu-labeled GRPR ligands incubated in human plasma at 37 °C for 72 ± 2 h, as analyzed by analytical radio-RP-HPLC (MultoKrom 100-5 C18, 5 μm, 125 × 4.6 mm, *CS Chromatographie GmbH*, Langerwehe, Germany; 20→35% MeCN in H_2O + 0.1% TFA in 20 min). (A) ^{177}Lu-RM2, (B) ^{177}Lu-NeoBOMB1, (C) ^{177}Lu-AMTG and (D) ^{177}Lu-AMTG2. Fractions representing intact compounds are indicated by black arrows (^{177}Lu-RM2: $K' = 8.7$, $t_R = 12.6$ min; ^{177}Lu-NeoBOMB1: $K' = 15.9$, $t_R = 22.0$ min; ^{177}Lu-AMTG: $K' = 9.9$, $t_R = 14.2$ min; ^{177}Lu-AMTG2: $K' = 11.5$, $t_R = 16.3$ min).
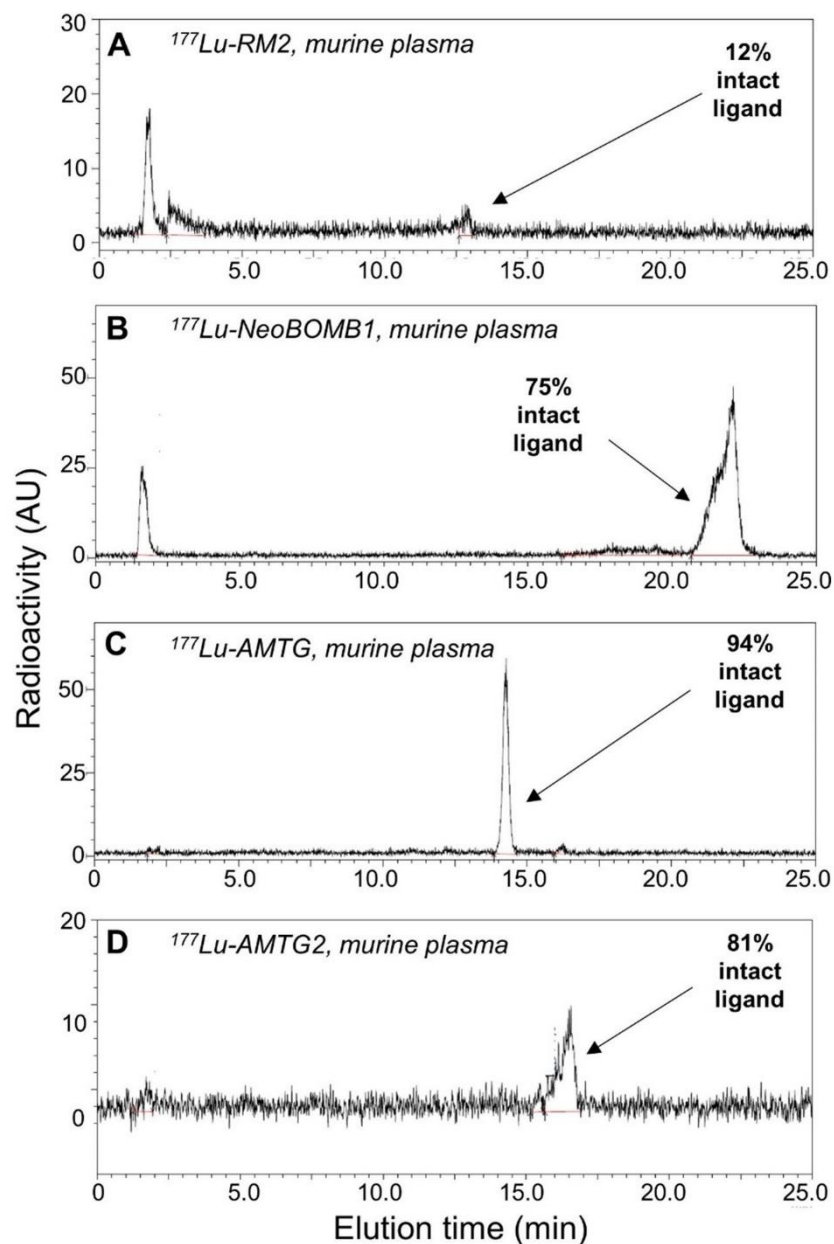
SUPPLEMENTAL FIGURE 15. *In vivo* stability of ^{177}Lu-labeled GRPR ligands in murine plasma (A-D) at 30 min p.i., as analyzed by analytical radio-RP-HPLC (MultoKrom 100-5 C18, 5 µm, 125 × 4.6 mm, CS Chromatographie GmbH, Langerwehe, Germany; 20→35% MeCN in H_2O + 0.1% TFA in 20 min). (A) ^{177}Lu-RM2, (B) ^{177}Lu-NeoBOMB1, (C) ^{177}Lu-AMTG and (D) ^{177}Lu-AMTG2. Fractions representing intact compounds indicated by black arrows (^{177}Lu-RM2: $K' = 8.7$, $t_R = 12.8$ min; ^{177}Lu-NeoBOMB1: $K' = 15.9$, $t_R = 22.9$ min; ^{177}Lu-AMTG: $K' = 9.9$, $t_R = 14.5$ min, ^{177}Lu-AMTG2: $K' = 11.5$, $t_R = 16.6$ min).
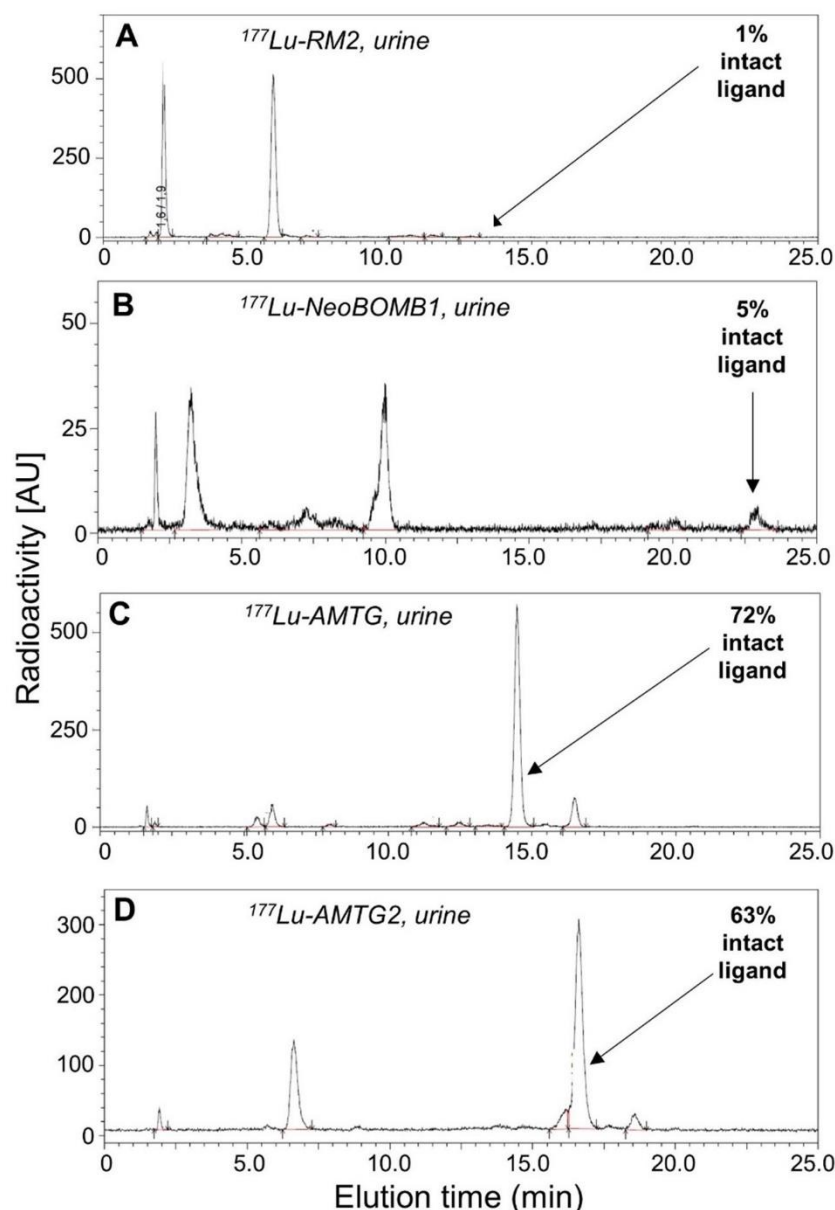
SUPPLEMENTAL FIGURE 16. *In vivo* stability of ^{177}Lu-labeled GRPR ligands in murine urine (A-D) at 30 min p.i., as analyzed by analytical radio-RP-HPLC (MultoKrom 100-5 C18, 5 μm, 125 × 4.6 mm, CS Chromatographie GmbH, Langerwehe, Germany; 20→35% MeCN in H$_2$O + 0.1% TFA in 20 min). (A) ^{177}Lu-RM2, (B) ^{177}Lu-NeoBOMB1, (C) ^{177}Lu-AMTG and (D) ^{177}Lu-AMTG2. Fractions representing intact compounds indicated by black arrows (^{177}Lu-RM2: $K' = 8.7$, $t_R = 12.8$ min; ^{177}Lu-NeoBOMB1: $K' = 15.9$, $t_R = 22.9$ min; ^{177}Lu-AMTG: $K' = 9.9$, $t_R = 14.5$ min, ^{177}Lu-AMTG2: $K' = 11.5$, $t_R = 16.6$ min).
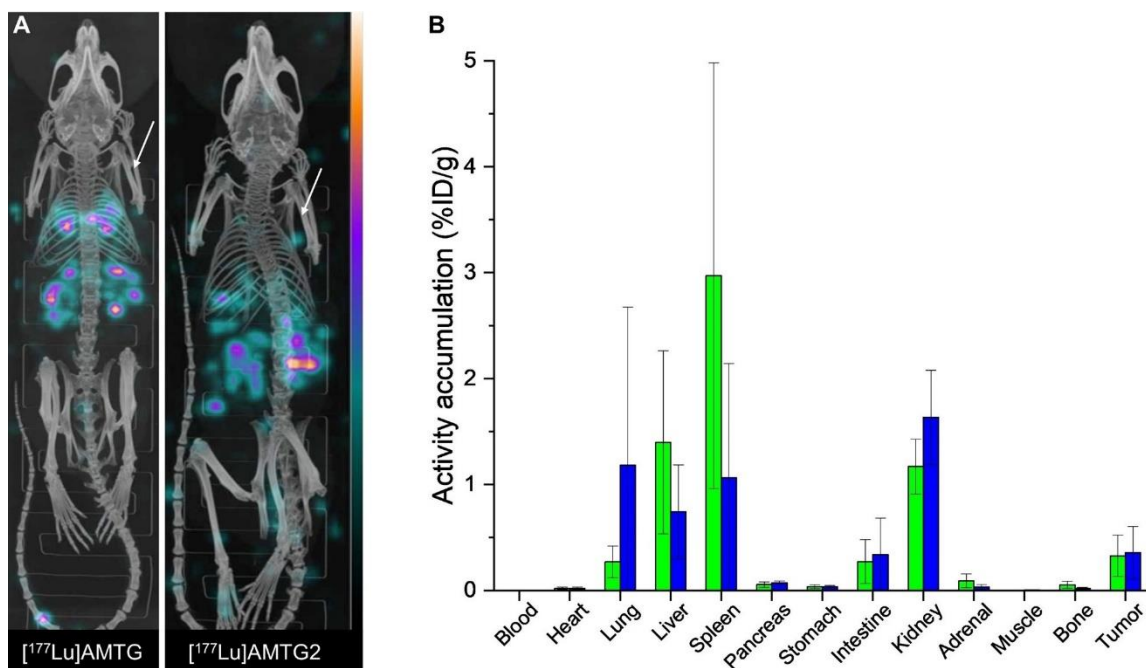
SUPPLEMENTAL FIGURE 17. (A) Maximum intensity projection of PC-3 tumor-bearing CB17-SCID mice injected with each 100 pmol of ^{177}Lu-AMTG (left) and ^{177}Lu-AMTG2 (right) and co-injected with an excess of ^{nat}Lu-RM2 (3.62 mg/kg). Images were acquired at 24 h p.i. PC-3 tumors are depicted by white arrows; (B) Biodistribution of ^{177}Lu-AMTG (green) and ^{177}Lu-AMTG2 (blue) co-injected with an excess of ^{nat}Lu-RM2 (3.62 mg/kg) in selected organs (in %ID/g) at 24 h p.i. in PC-3 tumor-bearing CB17-SCID mice (100 pmol each). Data is expressed as mean ± SD (n = 3).
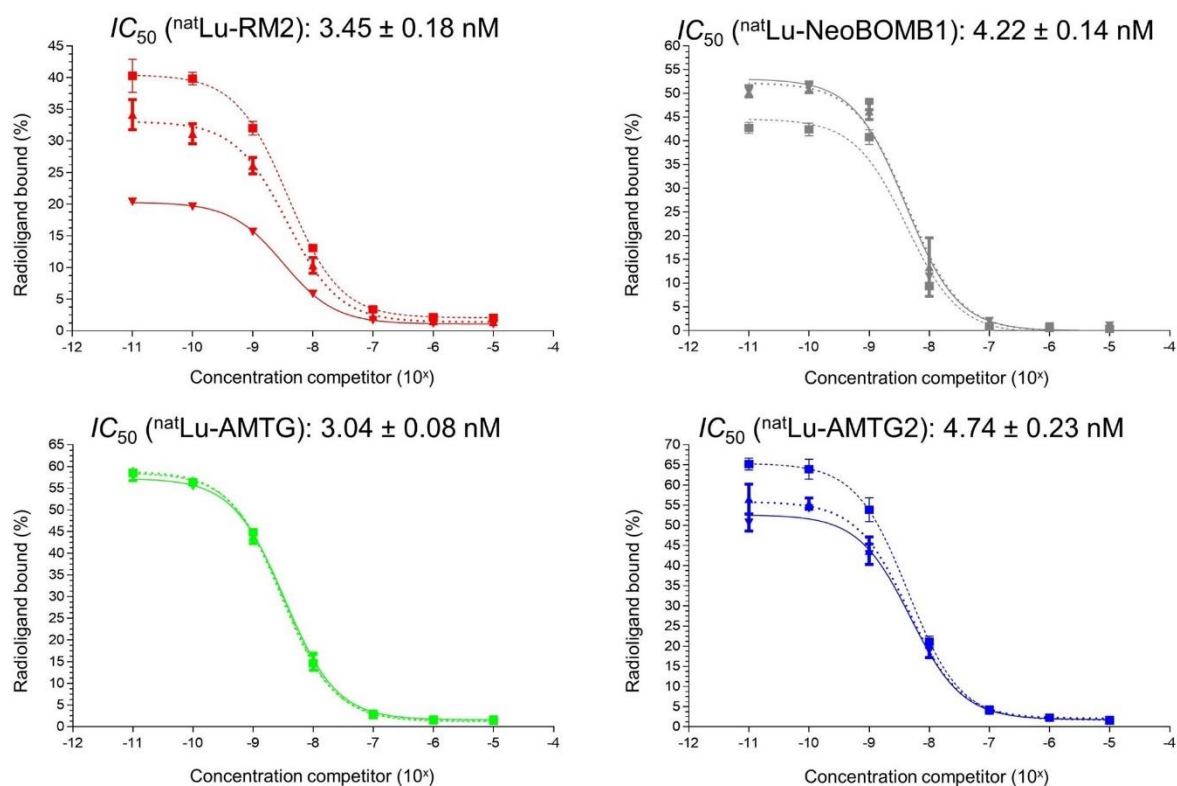
SUPPLEMENTAL FIGURE 18. Sigmoidal binding curves and calculated mean IC_{50}´s as obtained by competitive binding studies of ^{nat}Lu-RM2, ^{nat}Lu-NeoBOMB1, ^{nat}Lu-AMTG and ^{nat}Lu-AMTG2. Binding studies have been carried out in triplicate, using 1.5×10^5 PC-3 cells/ml/well, rt, 2 h; using 3-^{125}I-D-Tyr^6-MJ9 (0.2 nM/well) as radiolabeled reference (n = 3).
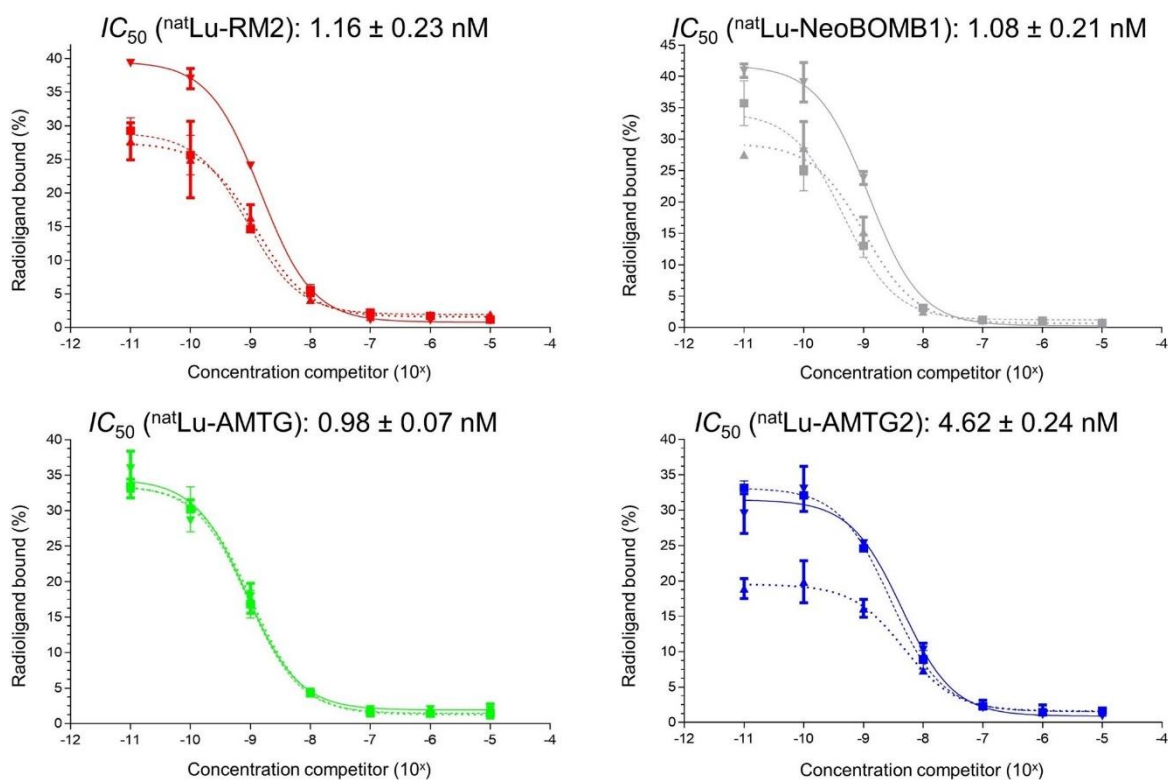
SUPPLEMENTAL FIGURE 19. Sigmoidal binding curves and calculated mean IC_{50}´s as obtained by competitive binding studies of natLu-RM2, natLu-NeoBOMB1, natLu-AMTG and natLu-AMTG2. Binding studies have been carried out in triplicate, using 1.5×10^5 T-47D cells/ml/well, rt, 2 h; using $3\text{-}^{125}\text{I-D-Tyr}^6\text{-MJ9}$ (0.2 nM/well) as radiolabeled reference (n = 3).